Measurement 253 (2025) 117810

Contents lists available at ScienceDirect

Measurement

journal homepage: www.elsevier.com/locate/measurement

Data reconstruction leverages one-dimensional Convolutional Neural Networks (1DCNN) combined with Long Short-Term Memory (LSTM) networks for Structural Health Monitoring (SHM)

T.Q Minh [a], Jose C. Matos [a], Helder S. Sousa [a], Son Dang Ngoc [a], Thuc Ngo Van [b], Huan X. Nguyen [c,d], Quyền Nguyễn [e,*]

[a] ISISE, ARISE, Department of Civil Engineering, University of Minho, 4800-058 Guimarães, Portugal
[b] Mien Tay Construction University, Vinh Long 85100, Vietnam
[c] London Digital Twin Research Centre, Middlesex University, London NW4 4BT, UK
[d] International School, Vietnam National University, Hanoi, Vietnam
[e] 2C2T-Centro de Ciência e Tecnologia Têxtil, Universidade do Minho, 4800-058 Guimarães, Portugal

ARTICLE INFO

Keywords:
Data reconstruction
Neural network-based methods
Hybrid 1DCNN-LSTM
Structural health monitoring

ABSTRACT

SHM data collected in systems often face data loss due to transmission errors, sensor damage, or environmental impacts. Incomplete data can lead to erroneous assessments in evaluating structural safety in complex structures. Although data reconstruction has been studied, challenges are present in data reconstruction: (i) SHM data contains a large amount of noise; (ii) data structure is complex and doesn't allow for simple linear or nonlinear formulation; (iii) reconstructed data needs to be accurate and reliable. This study proposes a hybrid deep learning approach combining the 1DCNN and LSTM network to reconstruct data within an SHM environment. The proposed model uniquely leverages 1DCNN for efficient spatial feature extraction and LSTM for capturing long-term temporal dependencies. Input data is strategically preprocessed through correlation-based sensor clustering and time-shift enhancement techniques. A hybrid model used the SHM data measurements before data loss to train models. The trained hybrid network can then reconstruct missing or erroneous data. The proposed method is validated on real datasets from different structures in various scenarios and can be applied in practice, achieving better performance and accuracy compared to other neural network-based methods. Quantitative results show that the hybrid model reduces the Mean Absolute Error (MAE) by 10–15% and achieves Modal Assurance Criterion (MAC) values exceeding 0.95, outperforming other baseline neural network models. These results highlight the model's practical applicability for accurate SHM data reconstruction under both single- and multi-channel sensor failures.

1. Introduction

1.1. Data loss in SHM

A Structural Health Monitoring (SHM) system plays a significant role in ensuring the safety and sustainability of bridges, especially complex ones [1,2]. Using sensors and measuring devices, SHM provides real-time bridge monitoring and allows condition assessment. Thus, signs of surface deterioration or damage can be detected and, if properly deployed, also inside the structure (e.g., cracks, deformation, corrosion). In that scenario, early detection of an issue allows bridge management responsible for identifying hazards and preventing potential incidents [3]. Additionally, SHM integrated with predictive models can support decisions on bridge interventions such as repair, maintenance, or strengthening when necessary. For large bridge structures, any failure can cause serious damage and consequences. Thus, the implementation of SHM systems is essential.

An SHM system consists of many sensors and devices integrating different technologies. They are installed at specific locations to collect essential data for structural health diagnosis [4–6]. By combining various sensors and measuring devices, the SHM system can provide a comprehensive and detailed representation of the bridge's condition, thereby supporting the safe and optimized maintenance, management, and operation of the bridge. The above results benefit from the real-time

* Corresponding author.
E-mail address: quyen@2c2t.uminho.pt (Q. Nguyễn).

https://doi.org/10.1016/j.measurement.2025.117810
Received 6 November 2024; Received in revised form 9 April 2025; Accepted 7 May 2025
Available online 10 May 2025

data source of the SHM system. The data of the SHM system plays an essential role, being the foundation for analysis and evaluation [7,8]. Data from sensors is processed and analyzed by experts. From the theoretical background and the analysis results, the condition of the structure is discerned [9]. Maintenance and upgrade strategies that are reasonable and effective, optimizing costs and resources, will be planned based on structural assessments from the SHM system. In other words, from the SHM system's data, engineers will aim to preserve the bridge structure in a safe condition state. Moreover, in case of any damage, the losses will be minimized [10]. In addition, historical and real-time data from the SHM system allows for the prediction of potential risks, thereby promoting predictive maintenance [11,12]. Through data collection and analysis, the SHM system not only helps maintain and enhance the safety of existing bridges but also contributes to the sustainable development of future transportation infrastructure [13].

SHM systems offer significant benefits in maintaining and managing bridges, from reducing the risk of sudden collapses to optimizing maintenance schedules. However, like any complex technology, SHM also faces various challenges such as unavailable and incomplete data, data management, timeliness, accuracy and source of truth, granularity and quality, and validation, among other parameters [14]. In this regard, data loss or errors, which is the most typical challenge, can be caused by different reasons, such as sensor equipment failure over long-term use or network connectivity issues. These problems are not just technical glitches but can significantly impact the effectiveness and safety of the SHM system. The SHM system heavily relies on the accuracy and continuity of the data collected from sensors and measuring devices [15]. When data is incomplete, the actual condition assessment of the bridge is severely affected, leading to ineffective maintenance strategies. On the other hand, misinterpretation of data might lead to delays in decision-making or even incorrect decisions in case of urgent disturbances, increasing the risk of safety incidents and waste of resources.

Several solutions have been proposed to address the issue of data loss or errors in SHM systems. On one hand, SHM systems are being upgraded with high-quality equipment [16]. On the other hand, regular inspections and calibrations are being conducted. In some cases, organizations employ preventive measures to protect data, such as backup storage, the use of secure data transmission protocols, and setting up alerts. Implementing redundant systems offers an additional layer of protection against data loss. For example, using multiple sensors for the same measurement can help verify if the sensors are working properly, verify the accuracy of the data, and identify any discrepancies. Intervention measures are implemented when issues arise, such as replacing sensors and repairing transmission lines. However, these solutions consume a significant amount of resources. In many cases, replacing or repairing components within the SHM system can be relatively complex, or even impossible. Sensors embedded within the system or deeply installed in the structure are difficult to repair or replace. Additionally, most SHM systems consist of homogeneous devices, and replacing them can lead to new issues.

Based on the above analysis, proposing data reconstruction solutions is essential. Data reconstruction solutions not only help overcome current limitations and shortcomings but also ensure the continuity and reliability of data in SHM systems, thus allowing for optimized resource management and system efficiency.

1.2. Data reconstruction: Related works

Over the past decades, numerous studies have attempted to propose solutions to deal with data errors and address data reconstruction issues. These solutions have applied diverse multidisciplinary technology and theory and achieved significant milestones. They can be categorized into four main groups: (i) data filtering/removal solution, (ii) statistical probability solution, (iii) model-based solution, and (iv) artificial intelligence solution.

The first group, data filtering/removal, is a simple method widely used in practice. It aims to delete outliers in data to facilitate subsequent analysis and achieve reliable results. The primary advantage of this solution relies upon its simplicity and ease of implementation. It does not require extensive computational resources and can be applied quickly to clean the data, smoothing the process for further analysis. However, excessive data removal can lead to the loss of important information and impact the final analysis results, particularly when dealing with heavy-tailed data distributions. Chen et al. [17] proposed a method for outlier removal termed Hankel-structured robust principal component analysis (HRPCA) to enhance the monitoring of structural dynamic responses. After applying this method, the dataset has been restored and utilized for monitoring. Also, Laencina et al. [18] reviewed several data removal methods in cases of missing or erroneous data, highlighting the advantages and disadvantages of these methods. Generally, the data removal methods tend to result in information loss and reduced reliability. However, they are highly effective in scenarios with abundant data and limited computational resources.

In the second group, statistical techniques are used to calculate and process missing or erroneous data. Missing or erroneous values can be replaced using different methods such as mean imputation, linear regression, or other statistical techniques [19]. These probabilistic statistical approaches are particularly effective with small datasets. They can quickly process and clean the data, ensuring consistency and accuracy in subsequent analyses. However, when applied to SHM systems with massive datasets (millions of data points per minute), these statistical methods become less effective. Processing such large amounts of data requires significant computational resources, leading to high costs and prolonged processing times. Furthermore, when dealing with such huge volumes of data, simple statistical methods can easily underperform, reducing the accuracy of the final results [18].

For the third group, model-based solutions, the simulation techniques are applied to create models that resemble real structures. Time series data can be recovered and generated using the development of numerical models. Shaikh and Nallasivam [20] used a finite element model (FEM) to simulate the dynamic response of a box girder bridge. While Zadel and Patnaik [21] modelled the dynamic response of a reinforced concrete composite bridge using FEM. Additionally, many other studies have used models to generate data for structural damage detection [22–25]. Model-based methods for data reconstruction offer certain efficiencies. However, the accuracy mostly depends on the simulation techniques and computational resources. In other words, they often omit some real-world conditions of the structure to simplify calculations, which can sometimes cause discrepancies in data reconstruction. The results may be acceptable for simple structures (such as simple supported bridges or short-span bridges), but for long-span bridges with complex structures (such as cable-stayed or suspension bridges) or multiple-span composite bridges, the results are often inaccurate. Additionally, the time-series data on structures are highly dependent on continuously changing environmental inputs (e.g., traffic density, wind loads, earthquakes, among others), causing the accurate replication very challenging.

The last group regards the applications of artificial intelligence. Recently the scientific revolution of Industry 4.0 has exponentially evolved with the development of artificial intelligence (AI) and powerful machine learning (ML) techniques. This has created favorable conditions for SHM in general and specifically for SHM data reconstruction. AI tools can learn from historical time-series data, recognize patterns, reconstruct, and predict data with high accuracy [26–29]. Simultaneously, ML techniques can effectively handle heterogeneous and noisy data, improving the reliability and quality of the reconstructed data. AI and ML have unlocked new possibilities in data reconstruction tasks, by automating data processing tasks, from noise filtering to analysis, enhancing efficiency and minimizing errors.

Overall, it can be stated that the AI and ML solutions in sensor data reconstruction tasks are very promising with high potential efficiency.

ML techniques are continuously being improved to keep up with the ever-growing data development. As the core of the ML technique, the Deep Learning (DL) algorithms are among the most promising for SHM data reconstruction tasks. Chen et al. [30] proposed the application of a deep learning and autoregressive (DL-AR) model to reconstruct strain data for SHM, taking into account the influence of thermal effects. Their results demonstrated that the proposed model achieved high performance and accuracy. In another study [31], convolutional neural networks (CNN) were introduced and applied to predict the long-term strain data of concrete structures. Furthermore, Lei et al. [32] presented a method using deep convolutional generative adversarial networks to reconstruct missing SHM data. Tang et al. [33] employed multivariate variational mode decomposition (MVMD) and fully convolutional networks (FCN) to reconstruct continuous data from a reinforced concrete arch and a real-world bridge. The results demonstrated the model's promising performance on acceleration data; however, its effectiveness was limited when the sensor channels lacked correlation. Additionally, the tested structures were relatively simple, indicating that the proposed method requires further development to handle more complex structural systems. Xin et al. [34] applied time-varying filtering-based empirical mode decomposition (TVFEMD), an encoder-decoder (ED) architecture, and a Long Short-Term Memory (LSTM) neural network to reconstruct SHM data from a suspension bridge. Their method achieved promising results; however, it did not take into account the spatial information related to the sensor locations during the data reconstruction process. Jiang et al. [35] used generative adversarial networks (GAN) to compute missing data points. This method showed promising results when tested with different scenarios. However, one of the limitations that needs to be overcome is the complexity of the model and the long training time. Li et al. [36] proposed a framework powered by multi-task Gaussian process regression to reconstruct dam SHM data. Although for single data reconstruction cases, the proposed framework has shown good performance, data loss scenarios across multiple sensors have not been considered. Recently, Wang et al. [37] proposed a hybrid model combining Kalman smoothing (Ks) and Long Short-Term Memory (LSTM) to impute missing wave height data. While this approach performed effectively for the studied dataset (wave data), it has not yet addressed the characteristics of SHM data, which involve both spatial and temporal features. Zhu et al. [38] proposed a method combining Wasserstein GAN with gradient penalty (WGAN-GP) and a U-Net generator to reconstruct missing SHM data. Although the proposed model achieves impressive results in data reconstruction, this study still has some limitations, such as a complex training system, difficulty to deploy in practice, the lack of ability to evaluate the reliability of reconstructed data, and missing continued data not considered. Wan and Ni [39] introduced a Bayesian multi-task learning framework for SHM data reconstruction. This study is limited in scenarios involving a large number of missing sensors, and various types of data loss cases have not been extensively investigated. Additionally, many other studies have demonstrated the potential and effectiveness of DL in SHM data reconstruction [40–44]. Although deep learning-based approaches have achieved certain successes in SHM data reconstruction, several aspects still require improvement. First, enhancing the accuracy of reconstructed data is essential, as higher accuracy leads to better performance of SHM systems. Second, the proposed models should be adaptable to various missing data scenarios, including single-point loss, multi-point loss, and data loss at multiple sensor locations. In addition, the reconstruction methods should be simplified and possess high interpretability to improve the reliability of the results. It is also important for these approaches to consider both the temporal and spatial characteristics of SHM data. Finally, the applicability of the algorithms should be further improved to handle more complex structural systems [45].

The present work proposes a hybrid model combining one-dimensional convolutional neural networks (1DCNN) and Long Short-Term Memory networks (LSTM) for sensor data reconstruction. This approach offers potential solutions to the aforementioned challenges. Firstly, 1DCNN-LSTM hybrid model uses the robust features of both 1DCNN and LSTM for time-series sensor data reconstruction tasks. Specifically, 1DCNN excels in learning and extracting data features, while LSTM can retrieve information over long periods, making it ideal for time-series data. This helps enhance the accuracy of the reconstructed data. Secondly, the model demonstrates flexibility across various missing data scenarios, including single-point loss, multi-point loss, and spatially distributed sensor loss. Moreover, compared to more complex architectures, the 1DCNN-LSTM framework is relatively lightweight and easily adaptable, contributing to improved interpretability and reliability. Importantly, this approach considers both the temporal and spatial characteristics of SHM data, which are crucial for realistic reconstruction. Finally, the model shows promising potential for application to complex structural systems, thereby enhancing its practicality and generalization capability. This is evidenced through two case studies: a laboratory-scale structure and a real-world large truss bridge.

The main contributions of this study include:

(1) *Strategic data preprocessing:* A novel preprocessing approach that leverages correlation-based sensor clustering and a time-shift enhancement technique. Unlike conventional methods that only use basic normalization or standardization, the preprocessing strategy intelligently restructures input data based on sensor correlations, thereby significantly reducing data complexity and enhancing model robustness. The application of time-shift data augmentation improves the model's ability to generalize effectively to unseen data scenarios, which is a substantial step forward from existing hybrid models that generally overlook or simplify preprocessing.
(2) *Customized hybrid architecture:* While previous studies typically apply general-purpose CNN-LSTM models without objective optimization, this study empirically determines the parameters through extensive experiments and systematic evaluation. This results in a highly efficient model that is particularly well-suited to SHM data reconstruction tasks. Specifically, the proposed model achieves up to a 15 % reduction in Mean Absolute Error (MAE), maintains Modal Assurance Criterion (MAC) values above 0.95 in both laboratory and real-world scenarios
(3) *Adaptability to complex data loss scenarios:* The study systematically evaluates the proposed hybrid model in various real-world data loss scenarios. The data tested range from laboratory structures to large real-world structures. Previous works have typically considered simpler scenarios or limited datasets. This study comprehensively validates and clearly demonstrates the model's capabilities in complex, real-world conditions.
(4) *Demonstrated superior performance:* The results demonstrate that the proposed hybrid model outperforms state-of-the-art neural network-based reconstruction methods, highlighting its efficiency and reliability. Across various scenarios, the 1DCNN-LSTM consistently achieved lower MAE, higher MAC values, and smaller modal frequency errors, especially in complex multi-channel data loss and high-noise environments. For example, while other models showed MAC values dropping below 0.93 under challenging conditions, the proposed model maintained MAC values above 0.98 in most single-channel cases and above 0.95 in moderate multi-channel loss scenarios.

This paper is organized into four main chapters: Introduction, Research Methods and Approach, Case Studies, and Conclusion. The Introduction starts to discuss the motivation and related research on data reconstruction in SHM, and it is followed by the Research Methods chapter that presents the details of the hybrid 1DCNN-LSTM model and its implementation steps. Following, Case Studies are conducted and presented, and finally, key findings and contributions are highlighted in the Conclusion chapter.

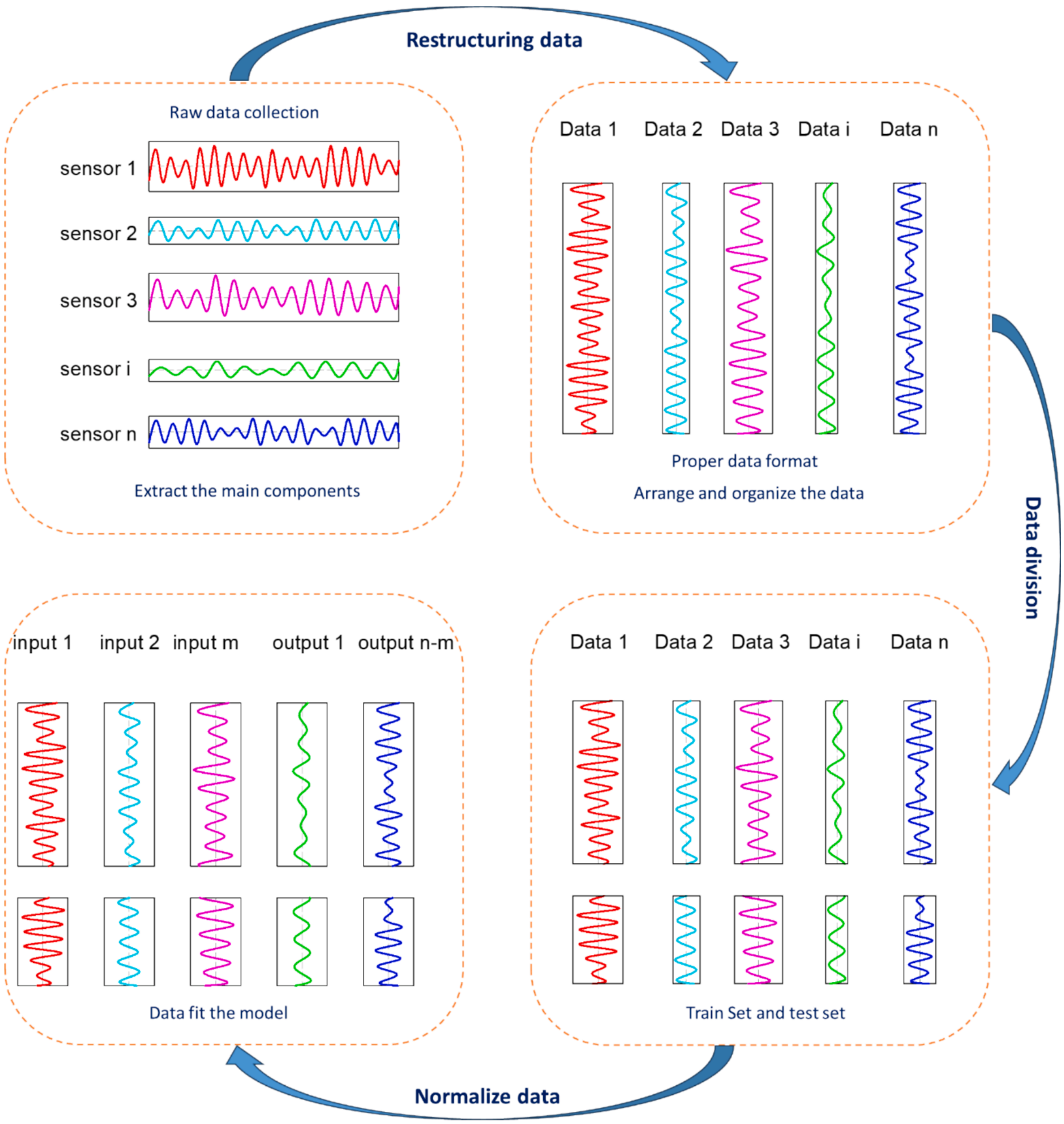

Fig. 1. Preprocessing data before feeding into the model.

2. Research methods and approach

2.1. Data gathering and preprocessing

Data in the SHM system takes the form of time series data, collected by sensors positioned on the structures. This data is continuously gathered in a specific chronological order; each data point is timestamped and typically has a high sampling frequency to ensure detail and accuracy.

Fig. 1 illustrates the data preparation process (or data preprocessing) before training the model for the task of data reconstruction. The complete raw data is collected from the sensors and stored. This data includes various information such as time, signals, number of channels, and sensor labels, among others. In the first step of data preprocessing, the data is separated to extract the main components, specifically the time-varying signals, while other components are processed accordingly to avoid redundancy. After extracting the main component of the data, a data matrix is constructed and mathematically represented as follows:

$$X = \{X^1; X^2; \dots; X^i; \dots; X^n\} \tag{1}$$

where n is the total number of sensors used to collect data, X is the overall matrix containing data from sensors, and X^i is the time series signal received by sensor number i.

To train a machine learning model, data needs to be restructured to meet the network's requirements, such as organizing input data, output data, and labels. Here, the raw data will be restructured to fit the requirements of the 1DCNN-LSTM architecture. This process involves applying matrix transformations to systematically and efficiently arrange and organize the data. After restructuring, the data will be divided into two parts, one part for training the model and another part for testing the model's accuracy and effectiveness. The training data will teach the model to learn important features and relationships within the data, enhancing the model's ability to make accurate predictions. The testing data, also known as the test set, will not be used during the training process but solely for evaluating the model's performance after training. This ensures that the model not only performs well on known data but also has the capability to generalize and make accurate predictions on new, unseen data. In this study, the training and testing sets will be split at a ratio of 70 % to 30 %. Using this 70/30 ratio ensures that

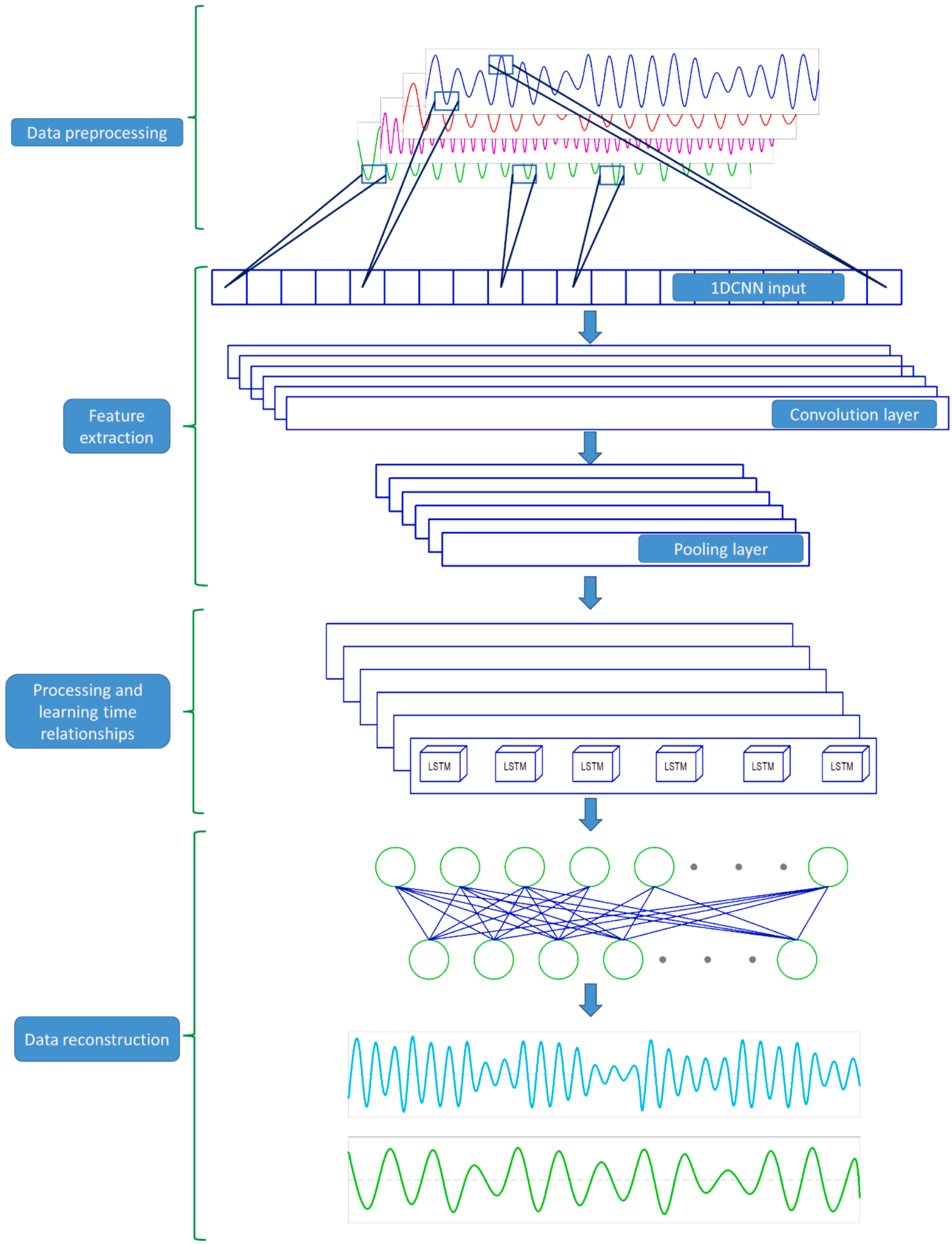

Fig. 2. Combining 1DCNN and LSTM networks for data reconstruction.

the model has enough data to learn effectively while retaining a significant portion of data to assess its accuracy and possibility for generalization. This approach promotes that the model not only performs well on known data but also accurately predicts new, unseen data.

The final step in data preprocessing is data normalization. This step ensures that all data is brought to a common standard, facilitating the training of the 1DCNN-LSTM model. When data features are standardized, the model can learn the important characteristics without being influenced by the differences in the scale of each feature. Normalization helps prevent the problem of overfitting because the model will not be excessively affected by extremely large or small values in the data that could be considered outliers. This makes the model training process more stable and the results more accurate. Data from the sensors is scaled to the range [0,1] using Min-Max Scaling (Equation (2)

$$x_{norm} = \frac{x - min(x)}{max(x) - min(x)} \tag{2}$$

where x_{norm} is the value after normalization, x is the value of the data being considered, and min*(x)* and max*(x)* are the minimum and maximum values of the data, respectively. At the end of the data preprocessing process, the data is saved and prepared for training the proposed model.

Data preprocessing in this study is carried out in a distinctive manner. This process optimizes the simultaneous exploitation of the 1DCNN's feature extraction capabilities and the LSTM's temporal data analysis strengths. A time-shift technique is applied to improve the model's generalization ability for SHM data. While conventional preprocessing methods typically involve basic normalization or standardization, this approach strategically restructures the data. After preprocessing, data leakage is carefully controlled, thereby enhancing the model's generalization and reliability in practical applications. Additionally, sensor data are grouped based on data correlation, reducing the complexity of information while improving its quality. This facilitates better performance of the proposed model.

2.2. Model architecture

2.2.1. 1DCNN

1DCNN [46] is a type of neural network that specializes in analyzing one-dimensional data, such as time-series signals from sensors [47]. The 1DCNN operates by sliding small filters over the input signal to automatically detect important patterns, like peaks, fluctuations, or trends. These patterns are then used as the basis for further processing and analysis [48]. Activation functions such as rectified linear unit (ReLU) and pooling layers then enhance and aggregate these features, reducing data dimensionality while retaining critical information. Finally, the extracted features are linked through fully connected layers to perform predictions or classifications. 1DCNNs not only improve classification performance but also serve as valuable tools in various applications such as time series analysis, audio recognition, and signal processing, effectively addressing challenges associated with sequential data processing.

The core operation in a 1DCNN is the convolution, which is defined as the scalar product of a filter (or kernel) with a sequence of data. Mathematically, the convolution of a sequence *x[i]* with a kernel *w[k]* is given by [49]:

$$y[i] = (x \times \mathrm{w})[\mathrm{i}] = \sum_{k=0}^{m-1} x[\mathrm{i} + \mathrm{k}].\mathrm{w}[\mathrm{k}] \tag{3}$$

where, *x[i]*is the input sequence (e.g., time series, signal), *w[k]* is the kernel or filter of size *m*, and *y[i]* is the output of the convolution operation, often referred to as the feature map.

2.2.2. LSTM

LSTM [50] network is a type of recurrent neural network (RNN) specifically designed to handle and learn from sequential data with long-term dependencies. ~~Unlike traditional RNNs,~~ LSTM networks overcome the vanishing gradient problem through their complex structure, which includes memory cells and gating mechanisms [51]. These mechanisms consist of forget, input, and output gates, each playing crucial roles in regulating the information retained, added, or output from the memory cell state. LSTM architecture allows the maintenance and update ofi nformation over long sequences, making them highly effective in applications requiring long-term dependency modeling, such as natural language processing, speech recognition, and time series prediction. This capability enables LSTMs to provide more accurate predictions and analyses for sequential data by retaining memory of past events and adjusting their state based on new inputs [48,52].

The memory cell is the core component of the LSTM, designed to store information over time. It can be updated, maintained, or forgotten based on the inputs received by the network [50]:

$$C_t = f_t \otimes C_{t-1} + i_t \otimes \widetilde{C}_t \tag{4}$$

where C_t is the memory cell state at time step *t*, f_t is the forget gate output at time step *t*, C_{t-1} is the memory cell state at the previous time step *t-1*, i_t is the input gate output at time step *t*, $\widetilde{C}_t$ is the candidate cell state, created by the input gate at time step *t*, and $\otimes$ is the element-wise multiplication

2.2.3. Combining 1DCNN and LSTM to reconstruct data

Combining 1DCNN and LSTM networks for data reconstruction leverages the strengths of both architectures to address complex time-series data challenges. The 1DCNN is adequate for extracting spatial features and patterns from sequential data and identifying important characteristics within individual time steps. Meanwhile, LSTM excels in capturing temporal dependencies and long-term relationships within the data, making it ideal for handling sequences where the order of events is crucial. This hybrid approach can reconstruct missing or corrupted sensor data with high accuracy, even in scenarios involving intricate patterns or dependencies. This combination is particularly effective in SHM, where both spatial and temporal information are critical, enabling more reliable data reconstruction and better structural integrity assessment over time. Fig. 2 shows the implementation steps of the proposed method.

After pre-processing, the data is stored as input matrices to be ready for training. The network's input is defined as the intact data, while the output corresponds to the data considered faulty or missing and requiring reconstruction. The data first passes through the 1DCNN layers to extract their features. The role of the 1DCNN layers is to identify and isolate important features, with the number of layers and parameters within each layer being customized according to the specific requirements of the problem at hand.

Once the features are extracted, they form data matrices containing distinct characteristics that reflect crucial aspects of the original data. These matrices are then fed into the LSTM layers for further training. LSTM specializes in handling temporal information, enabling the model to learn and recognize complex relationships between data points, including long-term dependencies that other models might overlook. Using LSTM, the model can effectively learn from time-series data, detecting repeating patterns and temporal variations, thereby enhancing the accuracy of data reconstruction.

Finally, the outputs are determined through the Fully Connected Layer. This layer synthesizes all the information processed and learned from the previous layers, converting it into the final output: accurately reconstructed data.

The mathematical interpretation of the process is presented below:

Input data

Assume the sensor signal collected is represented by a matrix:

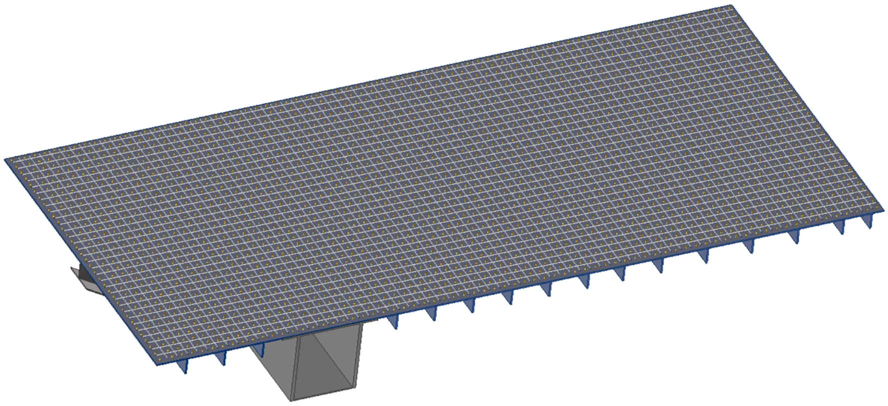

a.

b.

Fig. 3. A laboratory composite plate structure model: a: Structure design; b. The structure set in the laboratory and location in an onsite application [53].

$$\boldsymbol{X} = \begin{bmatrix} x_{1,1} & x_{1,2} & \cdots & x_{1,F} \\ x_{2,1} & x_{2,2} & \cdots & x_{2,F} \\ \vdots & \vdots & \ddots & \vdots \\ x_{T,1} & x_{T,2} & \cdots & x_{T,F} \end{bmatrix} \in \mathbb{R}^{T\times N} \quad (5)$$

where: T is the number of time steps; N is the number of sensors (input channels).

One-Dimensional Convolutional Layer (1DCNN).

a. Layer Parameters:

Number of filters: F.
Kernel size: k.
Kernel weights: $\boldsymbol{X}^{(c)} \in \mathbb{R}^{k\times N\times F}$
Bias vector: $b^{(c)} \in \mathbb{R}^{F}$

b. Operation:

At each time step t ∈{1,2,…,T-k + 1}, a sliding window segment is extracted from the input matrix:

$$\boldsymbol{X}_{t:t+k-1} = \begin{bmatrix} x_{t,1} & x_{t,2} & \cdots & x_{t,N} \\ x_{t+1,1} & x_{t+1,2} & \cdots & x_{t+1,N} \\ \vdots & \vdots & \ddots & \vdots \\ x_{t+k-1,1} & x_{t+k-1,2} & \cdots & x_{t+k-1,N} \end{bmatrix} \in \mathbb{R}^{k\times N} \quad (6)$$

For each filter f ∈ {1,2,…,F}, the convolution is computed as:

$$z_{t,f} = \sum_{i=1}^{k}\sum_{j=1}^{N} W^{(c)}_{i,j,f}\cdot x_{t+i-1,j} + b^{(c)}_{f} \quad (7)$$

The result is passed through a ReLU activation function:

$$h^{(1)}_{t,f} = max\left(0, z_{t,f}\right) \quad (8)$$

c. Output Matrix:

After applying all filters and scanning through time, the resulting output matrix is:

$$\boldsymbol{H}^{(1)} = \begin{bmatrix} h^{(1)}_{1,1} & h^{(1)}_{1,2} & \cdots & h^{(1)}_{1,F} \\ h^{(1)}_{2,1} & h^{(1)}_{2,2} & \cdots & h^{(1)}_{2,F} \\ \vdots & \vdots & \ddots & \vdots \\ h^{(1)}_{T',1} & h^{(1)}_{T',2} & \cdots & h^{(1)}_{T',F} \end{bmatrix} \in \mathbb{R}^{T'\times F} \quad \text{with } T' = T-k+1 \quad (9)$$

Long Short-Term Memory (LSTM) Layer.

a. Parameters:

Hidden state dimension: d.

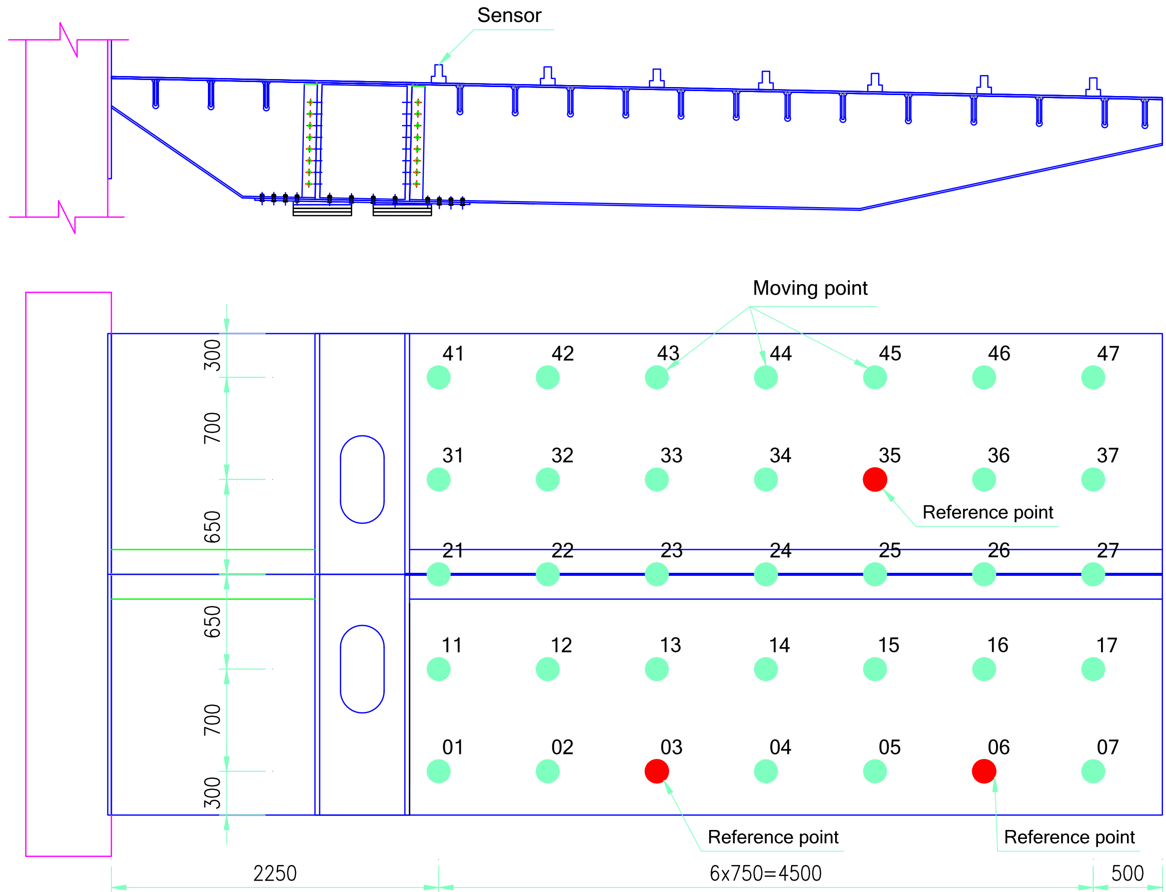

Fig. 4. Measuring grid designed for the experiment: red: reference point; cyan: moving point.

Input weight matrices:$W_i, W_f, W_o, W_c \in \mathbb{R}^{d\times F}$
Recurrent weight matrices:$U_i, U_f, U_o, U_c \in \mathbb{R}^{d\times F}$
Bias vectors:$b_i, b_f, b_o, b_c \in \mathbb{R}^d$

b. LSTM Computation at Each Time Step t ∈{1,2,…,T'}:

$h_t^{(1)} \in \mathbb{R}^F$ be the input at time t, and $h_{t-1}, c_{t-1} \in \mathbb{R}^d$ be the hidden state and cell state from the previous step. Then:

Input gate:

$$i_t = \sigma\left(W_i h_t^{(1)} + U_i h_{t-1} + b_i\right) \tag{10}$$

Forget gate:

$$f_t = \sigma\left(W_f h_t^{(1)} + U_f h_{t-1} + b_f\right) \tag{11}$$

Candidate cell state:

$$\tilde{c}_t = \tanh\left(W_c h_t^{(1)} + U_c h_{t-1} + b_c\right) \tag{12}$$

Cell state update:

$$c_t = f_t \odot c_{t-1} + i_t \odot \tilde{c}_t \tag{13}$$

Output gate:

$$o_t = \sigma\left(W_o h_t^{(1)} + U_o h_{t-1} + b_o\right) \tag{14}$$

Hidden state:

$$h_t = o_t.\tanh(c_t) \tag{15}$$

where: ⊙ is the Hadamard (element-wise) product, σ is the sigmoid activation function

c. Output Matrix:

$$H^{(LSTM)} = \begin{bmatrix} h_{1,1} & h_{1,2} & \cdots & h_{1,d} \\ h_{2,1} & h_{2,2} & \cdots & h_{2,d} \\ \vdots & \vdots & \ddots & \vdots \\ h_{T',1} & h_{T',2} & \cdots & h_{T',d} \end{bmatrix} \in \mathbb{R}^{T'\times d} \tag{16}$$

Fully Connected Layer for Output Prediction

a. Parameters:

Weight matrix:$W_{fc} \in \mathbb{R}^{d\times N'}$
Bias vector:$b_{fc} \in \mathbb{R}^{N'}$
N' is the number of sensor channels to be reconstructed.

b. Output at each time step t:

$$\hat{x}_t = h_t W_{fc} + b_{fc} \tag{17}$$

c. Final Output Matrix:

$$\hat{X} = H^{(LSTM)}.W_{fc} + 1_{T'\times 1}.b_{fc}^T \in \mathbb{R}^{T'\times N'} \tag{18}$$

Loss Function

Given the ground truth matrix $X_{true} \in \mathbb{R}^{T'\times N'}$, the model is trained by minimizing the Mean Squared Error (MSE):

$$\mathscr{L}_{MSE} = \frac{1}{T'\cdot N'}\sum_{t=1}^{T'}\sum_{j=1}^{N'}\left(x_{t,j}^{true} - \hat{x}_{t,j}\right)^2 = \frac{1}{T'\cdot N'}\|X_{true} - \hat{X}\|_F^2 \tag{19}$$

where $||.||_F$ denotes the Frobenius norm.

Fig. 5. Collecting vibration data of a composite plate structure model in laboratory conditions.

3. Testing and evaluating performance

3.1. A laboratory composite plate structure model

A full-scale cantilever model equivalent to the actual structure was constructed in the laboratory test bed (Fig. 3) within the Thang Long Bridge repair project (Hanoi, Vietnam) [53]. The experimental model aims to evaluate the current repair solution, while its data is used for research purposes in SHM.

The nominal dimensions of the model are $3.3 \times 7.25 \times 0.865$ m^3, which consists of the following components: a composite deck with support ribs, an I-section crossbeam, and a steel box beam (refer to Fig. 3). The composite deck consisted of a 14 mm steel plate reinforced with a UHPC coating layer with a thickness of 65 mm through stud connections. Underneath the deck, 16 steel support ribs are welded horizontally to enhance the stiffness and stability of the composite deck by countering the membrane effect. A transverse crossbeam with a variable I-section, which works in conjunction with a horizontal box beam, to support the entire composite deck and rib system. The highest I-section transverse crossbeam reaches up to 800 mm in height, while the horizontal box beam maintains a uniform height of 800 mm. In addition, two sets of steel bearings are placed under the box beam to transmit the load to the support base and to control a slope for the structure. In order to create a model with equivalent boundary conditions to the actual structure, steel anchors are used to anchor the test model to the laboratory side walls.

Data gathering.

An experimental dynamic test and data collection of the structural plate's acceleration response in the laboratory was conducted [54]. The equipment includes high-sensitivity accelerometers (PCB model sensors with a range of sensitivities from 1054 to 1083 mV/m/s^2), a converter and data acquisition system for the sensors, and a dedicated computer for data storage and processing. The surface of the structural plate was divided into a grid of square cells (measurement grid) to mark the locations for installing the accelerometers. The measurement grid comprises 35 points divided into 5 rows and 7 columns (Fig. 4).

Each grid point is marked and numbered to distinguish each other during the experiment. Due to the limitation of the number of sensors and input channels in the signal acquisition system, only 8 sensors corresponding to 8 measurement channels are used in each round of measurement. Therefore, the measurement test was performed by multiple sub-rounds, in which each sub-measurementconsisted of 3 reference points (which are fixed points and marked as numbers 03, 06, and 35), and five other points were selected from the remaining points.

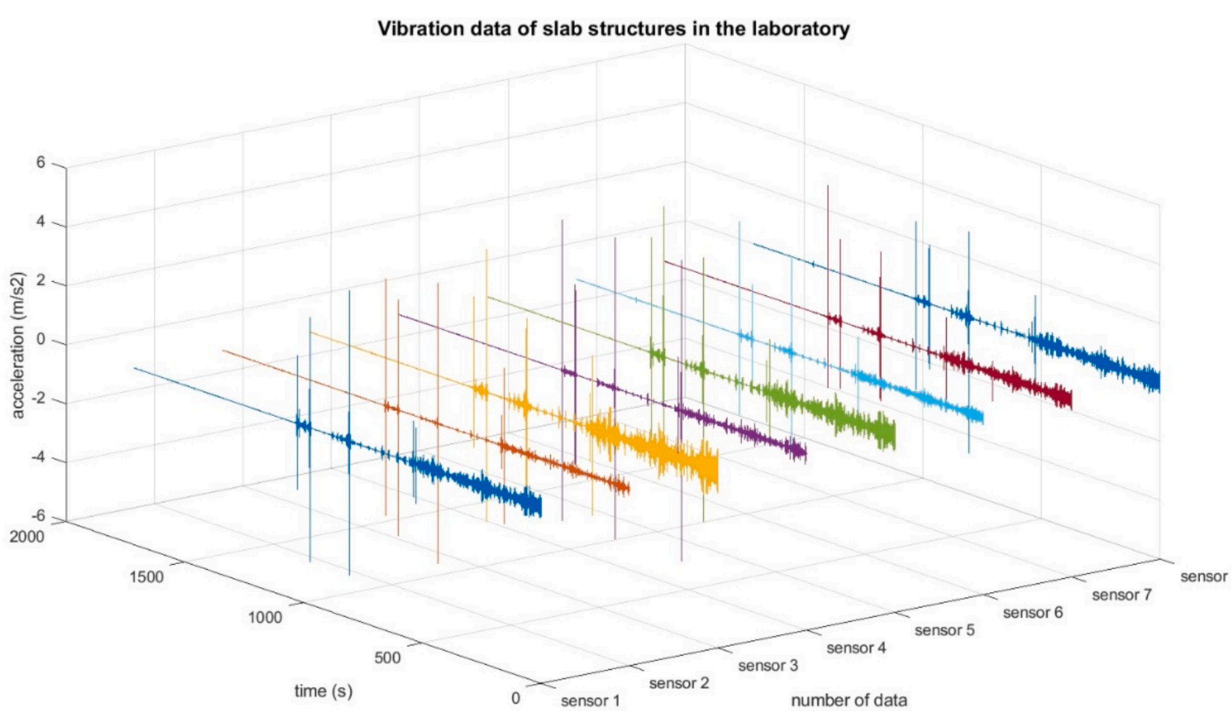

Fig. 6. Vibration data of slab structures in the laboratory in 1 sub-measurement.

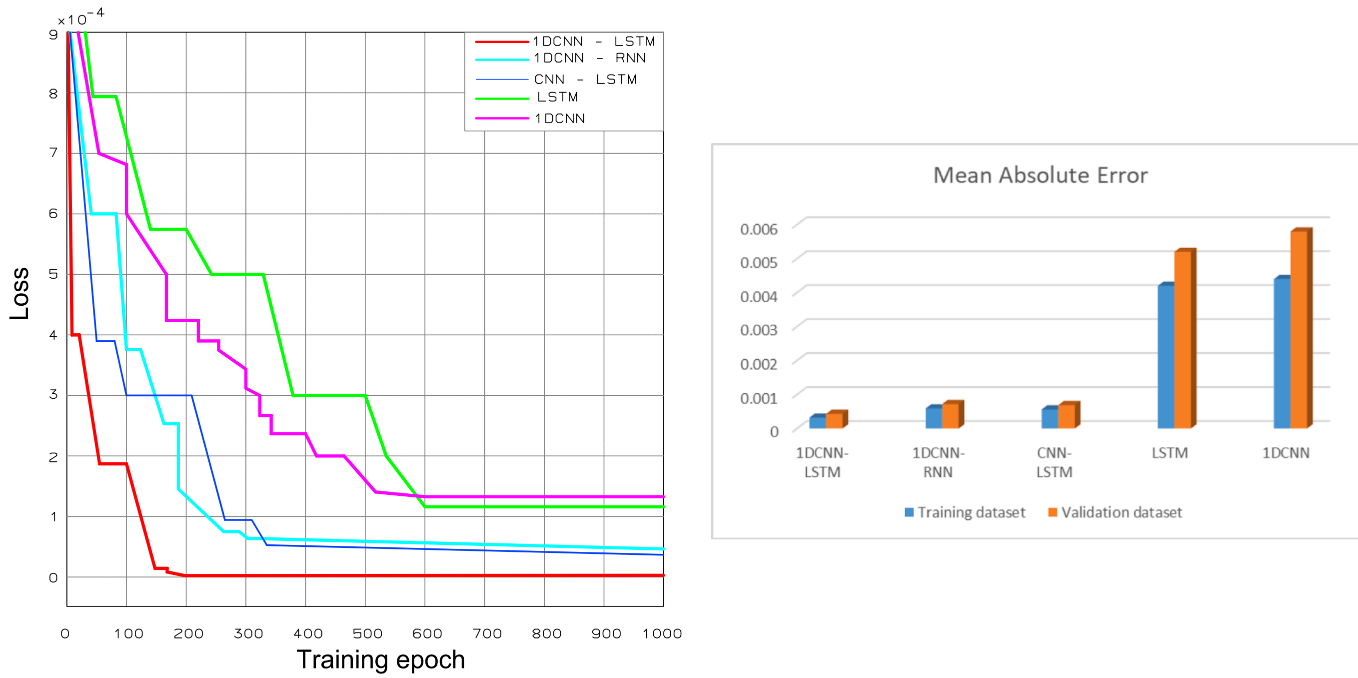

Fig. 7. Comparison of results between several machine learning models in data reconstruction: a. Loss training; b. Mean Absolute Error (MAE) of the best model.

Data from these sub-measurements was combined through the three reference points. The accelerometers are fixed on the surface of the plate at marked positions during the data collection of each sub-measurement. During the experiment, vibrational stimuli are generated by applying hydraulic force arranged above the plate structure (Fig. 5).

Data reconstruction

Fig. 6 shows the data collected in a sub-measurement. The acceleration values at the measurement points were continuously recorded over time with a sampling frequency of 1651 Hz (1651 samples per second). With a data collection period of approximately 40 min for each sub-measurement, the number of data points collected by a single sensor reaches nearly 4 million data points. The large amplitude segments in Fig. 6 were caused by controlled dynamic excitations applied using a hydraulic actuator to simulate sudden external loads.

3.1.1. *Single channel data loss*

In the first research scenario, a sensor malfunction is simulated, such that the data from one sensor becomes faulty and unusable. The other data remains intact, while the faulty sensor's data is assigned a value of 0 to indicate the error. The task of data reconstruction is then carried out.

The first step involves pre-processing the data from the sensors to prepare it for training the 1DCNN-LSTM model. Seven data columns corresponding to the data from seven sensors are identified as the input for the proposed model. Simultaneously, the output is the data from the sensor that needs to be reconstructed.

The proposed network combines three 1DCNN layers and four LSTM layers to perform the sensor data reconstruction. Each 1DCNN layer is equipped with 512 filters with a kernel size of 25 and the ReLU activation function. After the features have been extracted through the 1DCNN layers, the LSTM layers are used to process and analyze these features in a temporal sequence. These LSTM layers are particularly effective in handling time-series data, enabling the model to understand and predict trends and variations in the sensor data over time. In the first two LSTM layers, 512 memory cells are used, while the next two layers use 256 memory cells. After each LSTM layer, a "Dropout" layer with a parameter of 0.25 is employed. The purpose of the "Dropout" layers is to prevent overfitting and enhance the effectiveness of the training process. Fully connected layers are added at the end of the network, and the output is the data from the faulty sensor. The model compilation process is started. The model training is set to run for up to 1000 epochs, with a batch size of 30, using the Adam optimizer, a learning rate of 0.001, and the MSE loss function. The model with the best performance is then used to perform the data reconstruction task.

These parameter were determined based on a combination of literature references and empirical evaluation. Specifically, using three 1DCNN layers with 512 filters and a kernel size of 25 is inspired by studies that have successfully applied similar architectures to time series signal reconstruction tasks [31,33,41,42]. The kernel size of 25 was chosen after preliminary experiments with values ranging from 10 to 50 and it provides the best balance between local pattern detection ability and computational efficiency. Similarly, for LSTM, a four-layer stack was applied to increase the model's ability to learn long-term dependencies [40,48,49]. The memory cell size (512 for the first two layers and 256 for the last two layers) was selected through a grid search process to balance training performance and stability. Too large a memory cell size tends to cause overfitting in preliminary experiments. These parameters are selected after multiple tuning iterations, where variations in model depth, kernel size, and memory units are evaluated on a validation dataset. The selected configuration consistently yields the best reconstruction accuracy and MAC value metric performance.

Fig. 7 illustrates the training results of the proposed model alongside several other machine learning models in the task of data reconstruction [26,30,42,43]. Preliminary evaluations show that the 1DCNN-LSTM model has the best performance, surpassing other machine learning models (with the same parameters). Specifically, during the training of the 1DCNN-LSTM model, the convergence rate of the learning process is significantly faster than that of other models (Fig. 7a). The proposed model exhibits a rapid decrease in loss and converges close to zero by epoch 197. In contrast, other comparison models begin to converge around epoch 300 (for hybrid models) and even beyond 300 (for single models). The loss value of the 1DCNN-LSTM model is also the closest to zero. This indicates that the model achieves higher accuracy compared to the other models. The presence of plateaus in the training loss curve (Fig. 7a) occurs due to the complexity of SHM data. Additionally, this behavior results from the combination of non-stationary signals, dropout regularization, and the adaptive learning rate of the Adam optimizer. However, these short stagnation periods do not affect overall

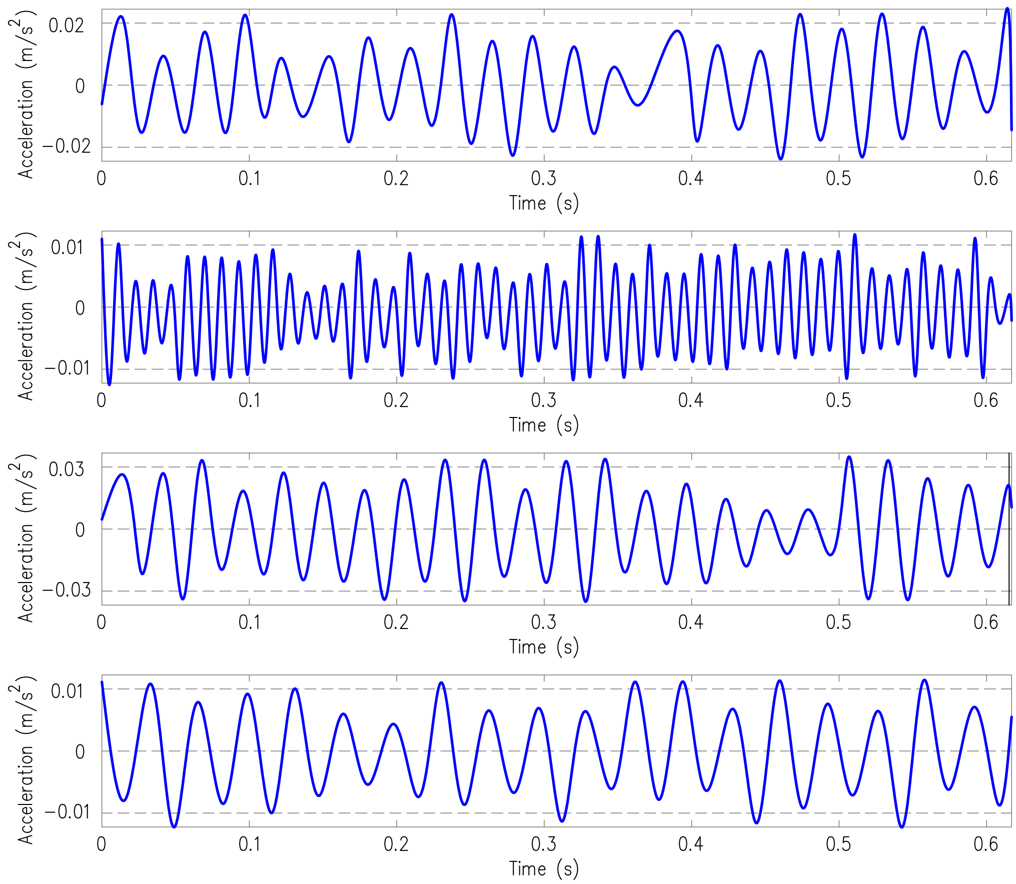

Fig. 8. Part of the data is reconstructed using different methods.

convergence and are consistent with the model's high reconstruction accuracy.

The mean absolute error between the reconstructed data values and the actual values in the training and testing sets of the models is shown in Fig. 7b. The 1DCNN-LSTM model has a very small error between the actual and reconstructed values, and it is the smallest among the models with the same configuration. This demonstrates that the 1DCNN-LSTM model can accurately and effectively reconstruct sensor data. Moreover, the error values in the training and testing sets for this model are quite similar, indicating that the model performs well and retains generalizability. The model performs well on known data and maintains high performance on new, unseen data.

Fig. 8 presents the reconstructed data results using various ML models. The data reconstructed using the 1DCNN-LSTM model closely aligns with the actual data. A detailed examination of Fig. 8 reveals that the 1DCNN-LSTM model consistently outperforms other models in accurately reconstructing the sensor data patterns. This is evidenced by the minimal deviation between the reconstructed data points and the actual values, indicating the model's higher ability to capture the underlying trends of the sensor data. In contrast, the other models exhibit more noticeable discrepancies, with some models showing significant deviations from the actual data, especially during periods of rapid change or fluctuation in the sensor readings. This highlights the robustness of the 1DCNN-LSTM model in handling complex data dynamics and maintaining high fidelity in data reconstruction. Although the reconstructed signals shown in Fig. 8 appear smooth, this is a typical result of neural network-based models, which tend to filter out noise while preserving key structural characteristics.

Two sets of reconstructed and actual data were input for analysis and comparison. After analyzing and processing the data using the MACEC toolbox [55]. Modal analysis was accomplished using the covariance-based stochastic subspace identification (SSI-COV) technique. The criteria used to concretize and characterize the modality frequency stabilization (1 %), damping ratio stabilization (5 %), and mode shape stabilization (1 %) [8]. The results are presented in Fig. 9 and Table 1.

The mode shapes obtained after analyzing the two datasets (reconstructed data and actual data) show similar patterns, indicating high accuracy in the data reconstruction process. These similarities demonstrate that the reconstructed data accurately reflects the dynamic characteristics of the system. Specifically, in the first two mode shapes, the vibration points nearly overlap, suggesting that the reconstruction model has accurately captured the primary mode shapes, which are crucial for understanding the structural response. It is particularly important in applications such as SHM, where the primary mode shapes play a significant role in assessing the condition and behavior of the structure. For the subsequent mode shapes, there are some points where the vibrations exhibit slight deviations, but these differences are not significant.

From the analysis results in Table 1 and Table 2, there is a discrepancy but not significant in the frequency values between the two datasets. The largest recorded discrepancy is in the fourth mode shape, with a deviation of 1.162 %. The Modal Assurance Criterion (MAC) values obtained when comparing the mode shapes also show high values, very close to 1. The highest MAC value is achieved in the second mode shape (0.997) and the lowest in the fourth mode shape (0.986). All MAC values are greater than 0.9, indicating high accuracy. The high MAC values further reinforce the effectiveness of the reconstruction model. The combination of minor differences in frequency values and high MAC values highlights the stability and reliability of the model in reconstructing sensor data.

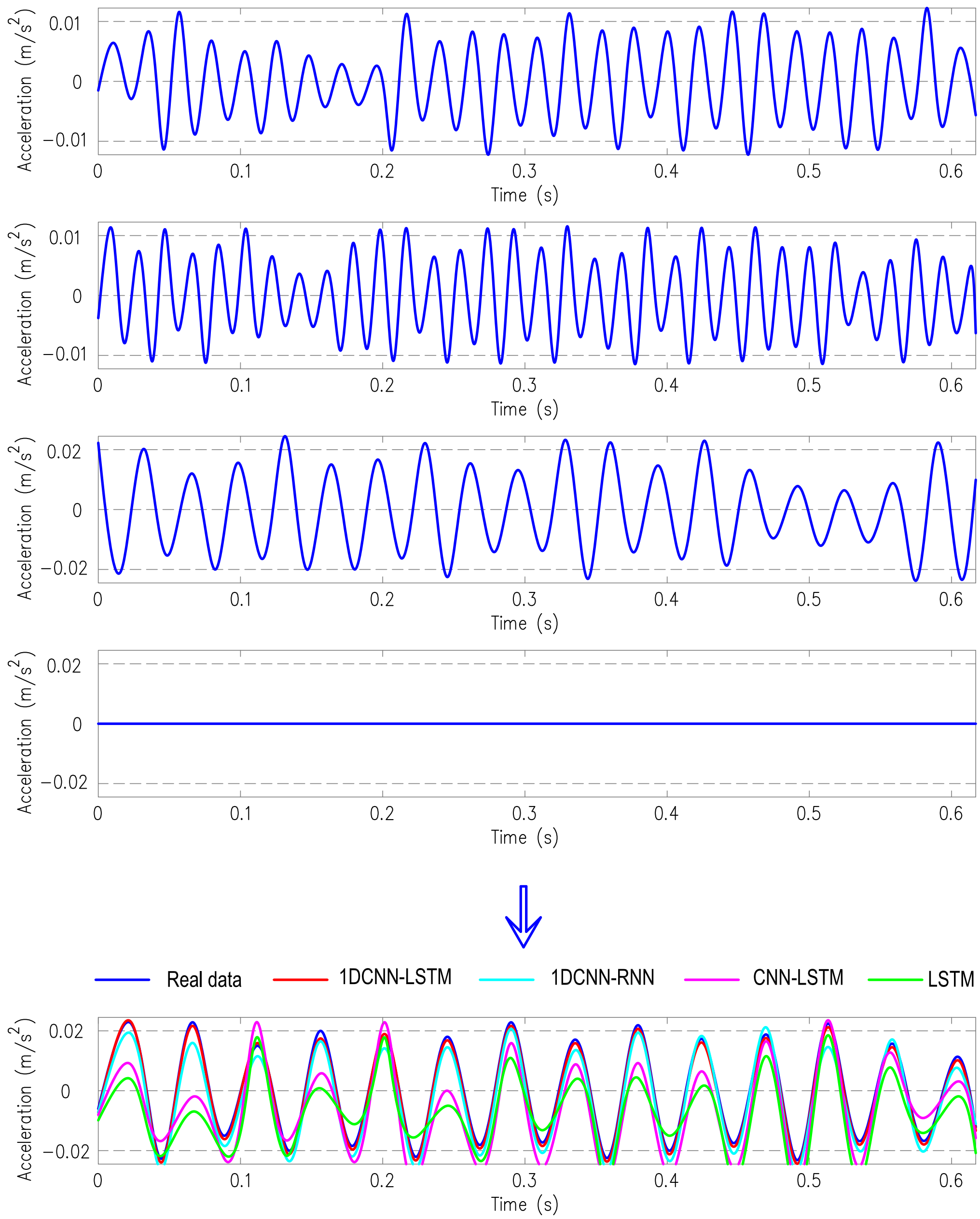

Fig. 8. (*continued*).

3.1.2. Multi-channel data loss

Various multichannel data loss scenarios were studied to determine the proposed method's effectiveness. This section will consider data loss scenarios ranging from 2 to 7 sensors. Correspondingly, the input of the trained network will vary from 6 to 1, and the output will vary from 2 to 7. This approach involves systematically reducing the number of input channels while increasing the number of output channels that the model needs to reconstruct. For instance, when data from 2 sensors is lost, the network will have 6 input channels and 2 output channels. Conversely, when data from 7 sensors is lost, the network will have only 1 input channel and 7 output channels. By examining these scenarios, the robustness and adaptability of the 1DCNN-LSTM model can be evaluated under different conditions of data loss. This comprehensive analysis ensures that the model's performance is thoroughly tested, providing insights into its capability to handle varying degrees of sensor data loss and still accurately reconstruct the missing data.

The parameters of the 1DCNN-LSTM model were selected similarly to the single-channel data loss scenario to ensure a consistent performance comparison. After preprocessing the data, the model's input and output were determined, and the training process commenced. Specifically, parameters such as the number of layers, number of filters, kernel size, activation function, learning rate, and loss function were kept the same as in the single-channel data loss scenario. The objective is to evaluate whether the model can maintain high performance when dealing with more complex data loss situations. During training, the model will learn to reconstruct the lost data from different sensor channels. Each scenario will be trained for a maximum of 1000 epochs with a batch size of 30, using the Adam optimizer and the MSE loss function. The training process and model performance will be closely monitored. Metrics such as MAE and MAC values will be calculated to assess the model's accuracy and reconstruction ability in each scenario. Fig. 10 presents the results of the proposed model training process.

The convergence curve of the training process is shown in Fig. 10a. In all cases, the convergence curve drops rapidly at the initial stage and then stabilizes horizontally. Preliminary evaluations indicate that the

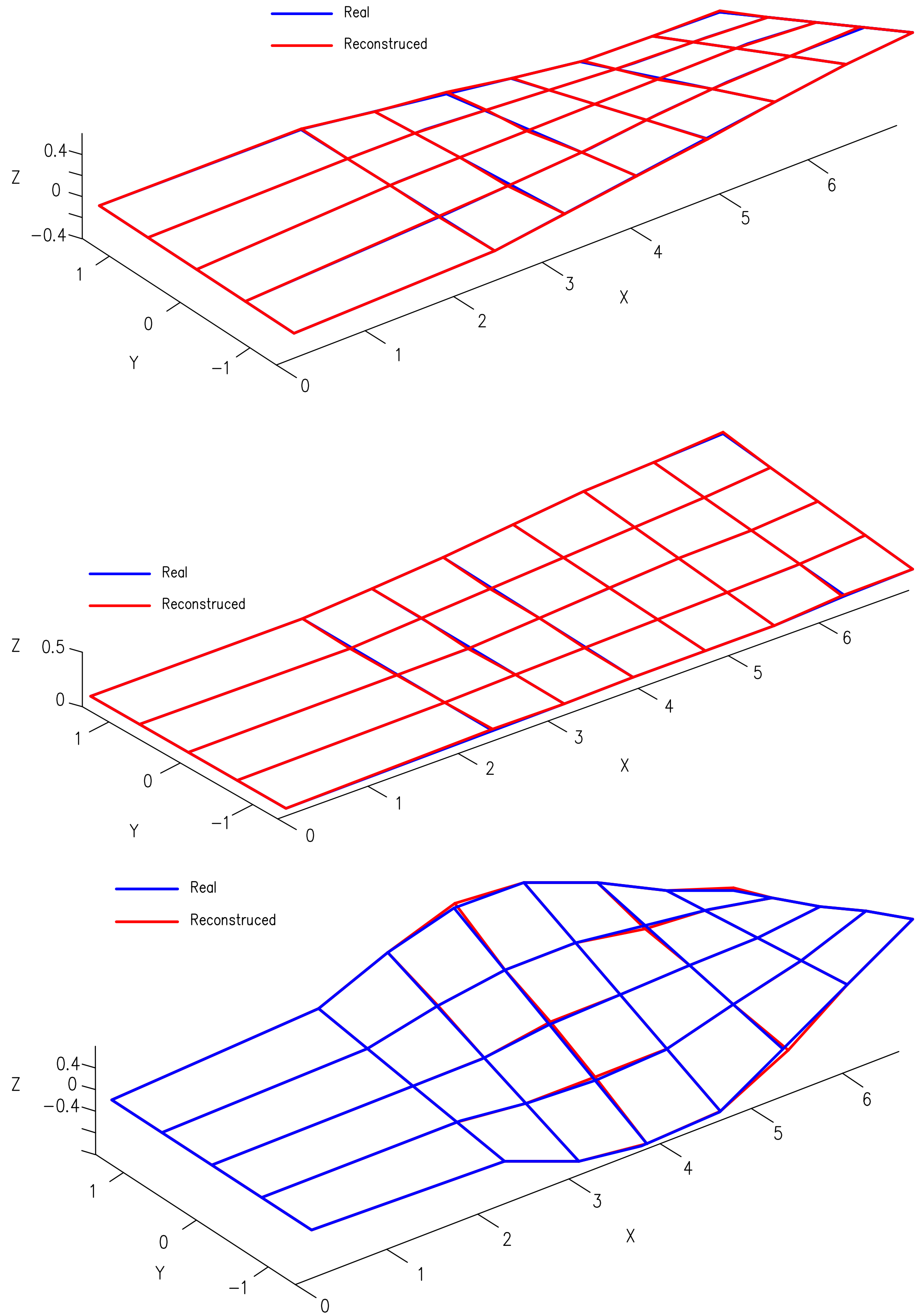

Fig. 9. Mode shape results of two real and reconstructed data sets: a. Mode 1: 1st torsion; b. Mode 2: 1st vertical bending; c. Mode 3: 2nd torsion; d. Mode 4: 2nd vertical bending; e. Mode 5: 3rd torsion (Compare with actual values in [8]).

method's efficiency decreases as the number of faulty sensors increases (input decreases and output increases). Specifically, when two faulty sensors need to be reconstructed, the model begins to converge and approaches the value of 0 within 249 epochs. As the number of faulty sensors increases, the number of epochs required for the model to converge also increases. In the case of 3 faulty sensors, the model starts to converge more slowly, requiring around 300 epochs to approach the value of 0. As the number of faulty sensors continues to increase to 4 and 5, the convergence time becomes even longer, indicating greater complexity and challenges in reconstructing data with decreasing input and increasing output.

However, in cases with 6 and 7 faulty sensors, although the model

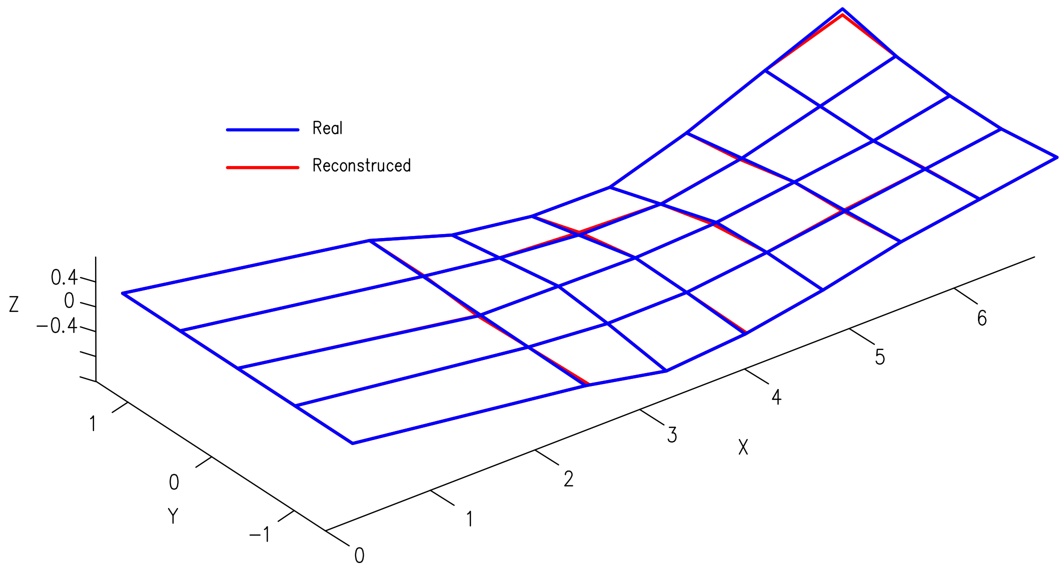

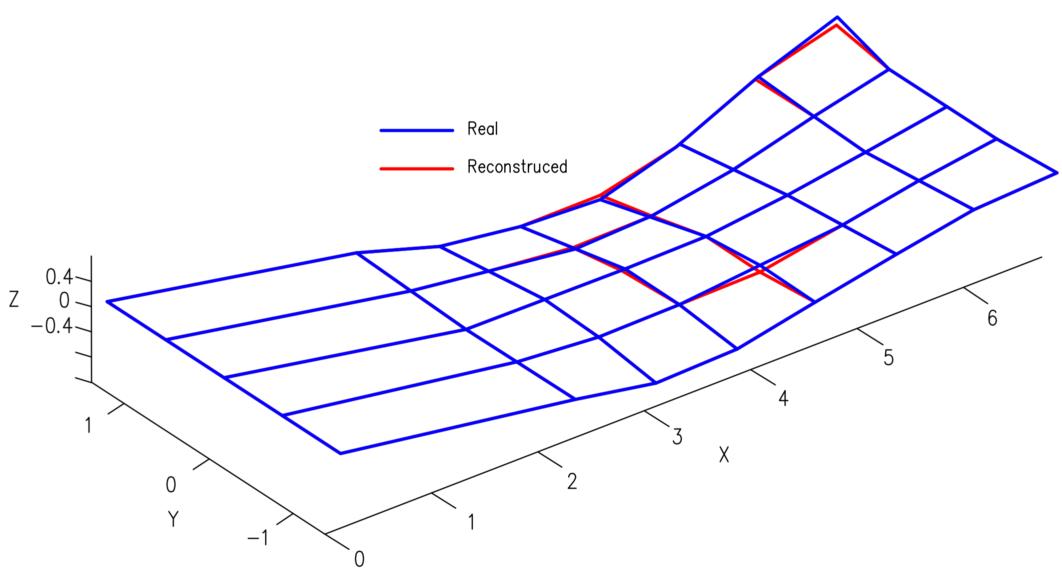

Fig. 9. (*continued*).

Table 1
Frequency analysis results of reconstructed datasets from different methods.

Mode	Real data	1DCNN-LSTM		1DCNN-RNN		CNN-LSTM		LSTM	
		f(Hz)	Error (%)	f(Hz)	Error (%)	f(Hz)	Error (%)	f(Hz)	Error (%)
1st	7.47	7.55	1.071	7.82	4.685	8.01	7.229	8.42	12.718
2nd	8.62	8.72	1.160	9.13	5.916	9.18	6.497	10.18	18.097
3rd	24.99	25.28	1.160	27.19	8.804	23.26	6.923	28.13	12.565
4th	36.16	36.58	1.162	38.53	6.554	39.12	8.186	31.46	12.998
5th	48.81	49.31	1.024	46.21	5.327	51.98	6.495	43.12	11.657

Table 2
MAC values of reconstructed datasets from different methods.

Mode	1DCNN-LSTM	1DCNN-RNN	CNN-LSTM	LSTM
1st	0.996	0.926	0.931	0.906
2nd	0.997	0.935	0.925	0.907
3rd	0.990	0.933	0.914	0.903
4th	0.986	0.942	0.934	0.900
5th	0.987	0.915	0.912	0.906

converges relatively quickly, the loss value does not tend to approach 0. This suggests that the model performs less effectively in these scenarios. The possible reason is that the model is insufficiently capable of learning and accurately reconstructing data when the amount of input information is too low and the amount of data to be reconstructed is too high in comparison. These results underscore that the model's effectiveness significantly diminishes when facing complex data loss situations with many faulty sensor channels, highlighting the need for further improvements and optimizations to enhance accuracy and data reconstruction capability in these challenging scenarios.

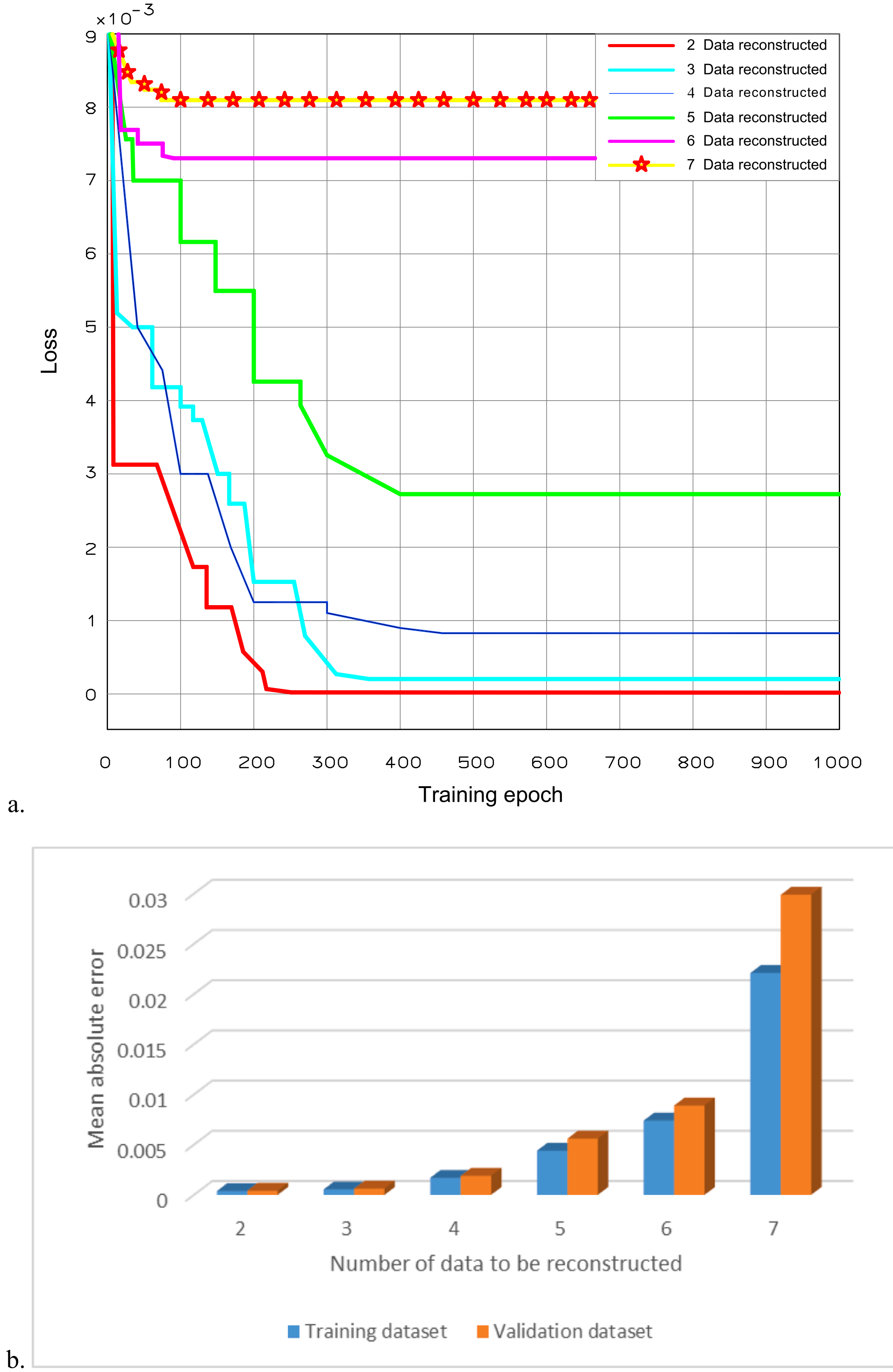

Fig. 10. Training results of the proposed mode: a. convergence curve; b. Mean absolute differences according to the number of data reconstruction.

Fig. 10b shows the mean absolute difference between the actual value and the reconstructed value based on the number of faulty sensors. The discrepancy between the actual value and the reconstructed value is smaller when the amount of data needing reconstruction is less. When only two sensors are faulty, the difference is negligible. However, this discrepancy gradually increases as the number of faulty sensors increases. Particularly, when the number of faulty sensors reaches five or more, the discrepancy increases significantly. This highlights the decline in the model's performance in accurately reconstructing data when dealing with a higher number of faulty sensors. It highlights the importance of having sufficient input data to maintain high accuracy in the reconstruction process and indicates that the model needs further improvement to handle more complex scenarios of data loss with multiple faulty sensors effectively. The MAC values were calculated to

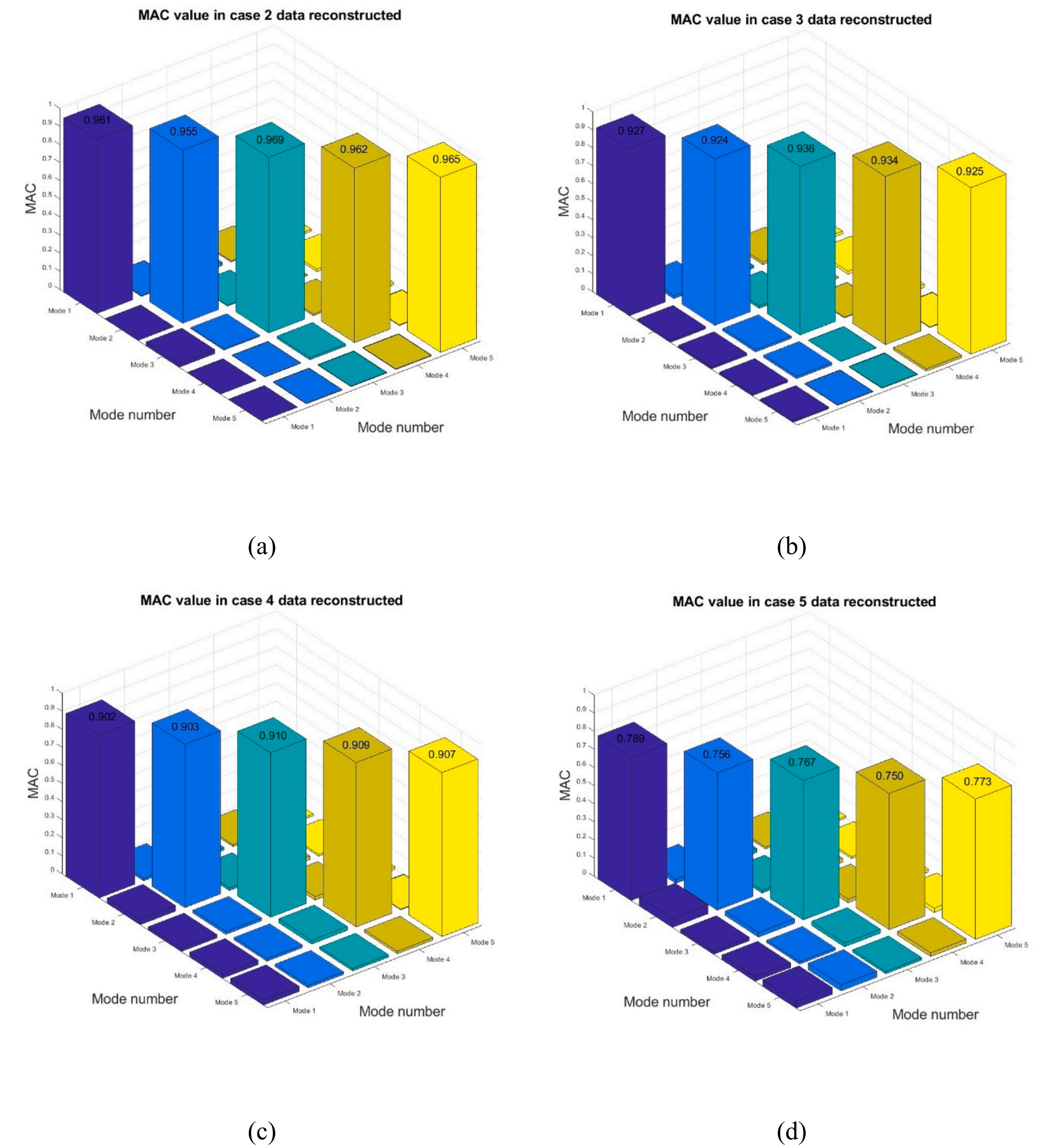

Fig. 11. MAC value in data loss scenarios.

evaluate the reconstructed datasets under different scenarios. Fig. 11 shows the MAC values for various sensor failure scenarios:

The reconstructed data showed relatively high MAC values in scenarios where 2 to 4 sensors failed. This was observed after the data was analyzed and compared with the mode shapes. Specifically, in cases where data had to be reconstructed from 2 to 4 failed sensors, the MAC values were all above 0.9. The MAC value matrix was relatively uniform. However, in scenarios where data needed to be reconstructed from 5 sensors (out of a total of 8), the method's effectiveness dropped significantly. This is consistent with previous evaluations of the model's effectiveness. For the scenario involving data reconstruction from 5 sensors, the highest MAC value achieved was only 0.789. This performance further decreased substantially in scenarios involving data reconstruction from 6 and 7 sensors, with MAC values reaching only

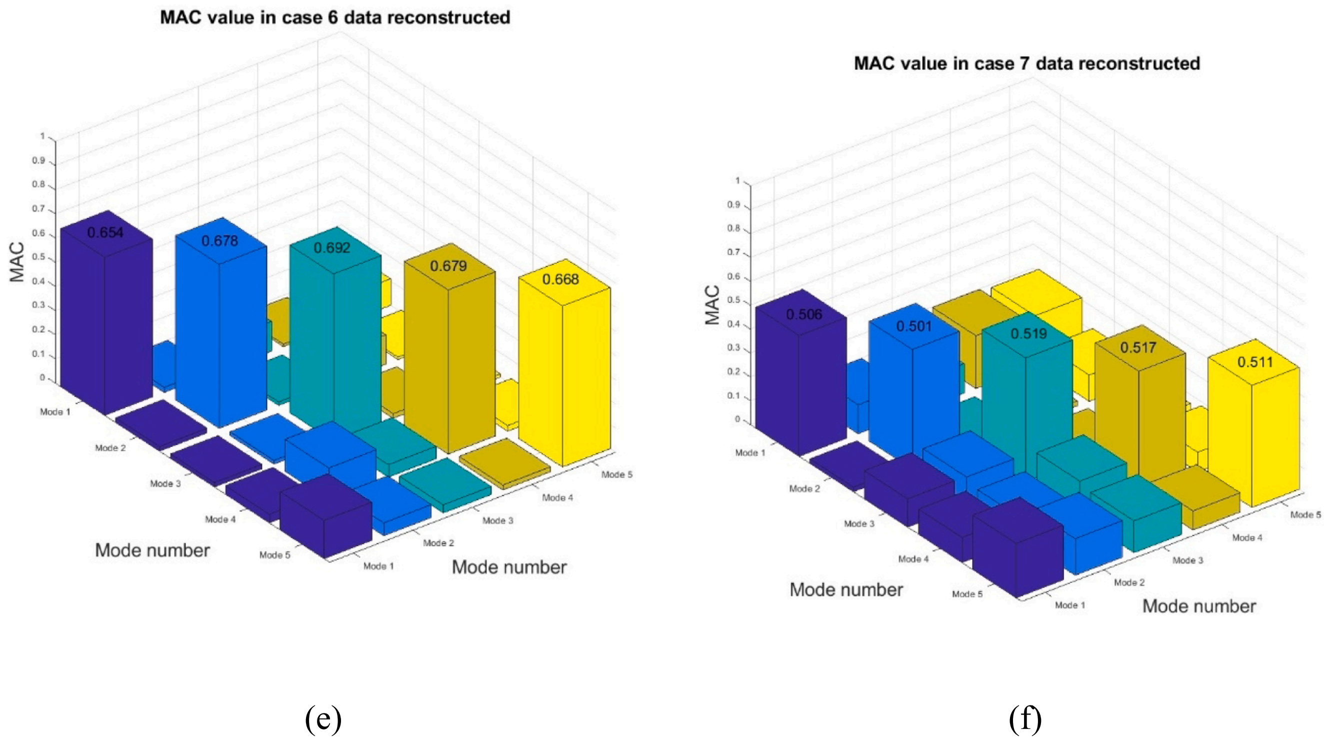

Fig. 11. (*continued*).

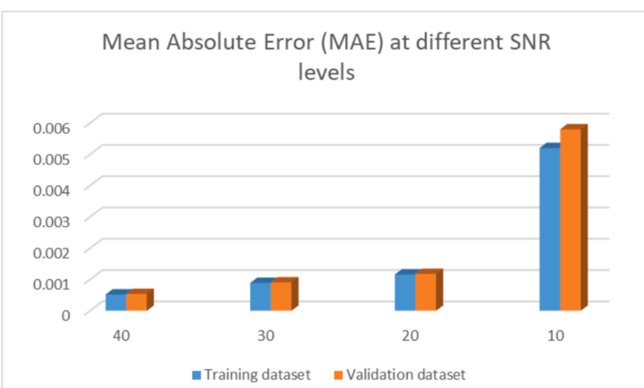

Fig. 12. Mean Absolute Error (MAE) of the best model at different SNR levels.

0.692 and 0.519, respectively. As the number of failed sensors increases, the model's ability to reconstruct data sharply decreases, highlighting the necessity for further improvement and optimization of the model to ensure accuracy in more complex situations.

3.1.3. Evaluation under different noise levels

In SHM systems, sensor signals are often subject to noise caused by the environment or hardware. It can degrade the performance of data-based models. An additional experiment was conducted to evaluate the impact of signal-to-noise ratio (SNR) on the accuracy of reconstructed data. This experiment allows for the evaluation of the reliability of the proposed solution when deployed in real-world conditions. The SNR analysis in this study focuses on a single-channel data reconstruction scenario to isolate the impact of noise on model performance. This allows for a clear assessment of how different levels of noise affect the accuracy of the reconstruction. Multi-channel data loss scenarios under noisy conditions will be explored in future studies.

Gaussian white noise was added to the laboratory dataset at different SNR levels. The noise levels considered were 40 dB (Signal is almost unchanged, noise is very small); 30 dB (Slight noise starts to appear, but signal is still clear); 20 dB (Noise becomes more visible, signal starts to distort slightly) and 10 dB (Signal is heavily noisy, waveform starts to be difficult to distinguish). These values represent increasing noise environments, with 40 dB representing minimal noise and 10 dB representing a high noise situation. The noise was added to all input sensor channels, while the actual output channel remained clean to simulate real-world reconstruction conditions. The 1DCNN-LSTM architecture and training parameters were used in the single-channel reconstruction scenario. This ensures that the observed variations in reconstruction accuracy are due only to added noise and not to changes in architecture or hyperparameters.

Table 3
MAC at different SNR levels.

SNR (dB)	Mode 1	Mode 2	Mode 3	Mode 4	Mode 5
40	0.991	0.990	0.986	0.983	0.984
30	0.976	0.968	0.962	0.967	0.959
20	0.938	0.926	0.910	0.912	0.901
10	0.872	0.855	0.837	0.825	0.801

The data reconstruction results considering the SNR levels are shown in Fig. 12 and Table 3:

The proposed model maintains high MAC values (>0.9) and low MAE up to 20 dB, indicating that it is robust against moderate noise levels. At 10 dB, the performance degrades more significantly, which is expected due to the significant noise in the input signals. These results confirm that the 1DCNN-LSTM model can still produce reliable reconstructions under typical noise conditions in SHM, reinforcing its practical applicability.

3.2. Practical applications – Chuong Duong truss bridge

Chuong Duong Bridge (Fig. 13) is located in Hanoi, Vietnam, serving as a vital transportation link across the Red River. The main bridge spans

Fig. 13. Chuong Duong Bridge: a. side view; b. in front view.

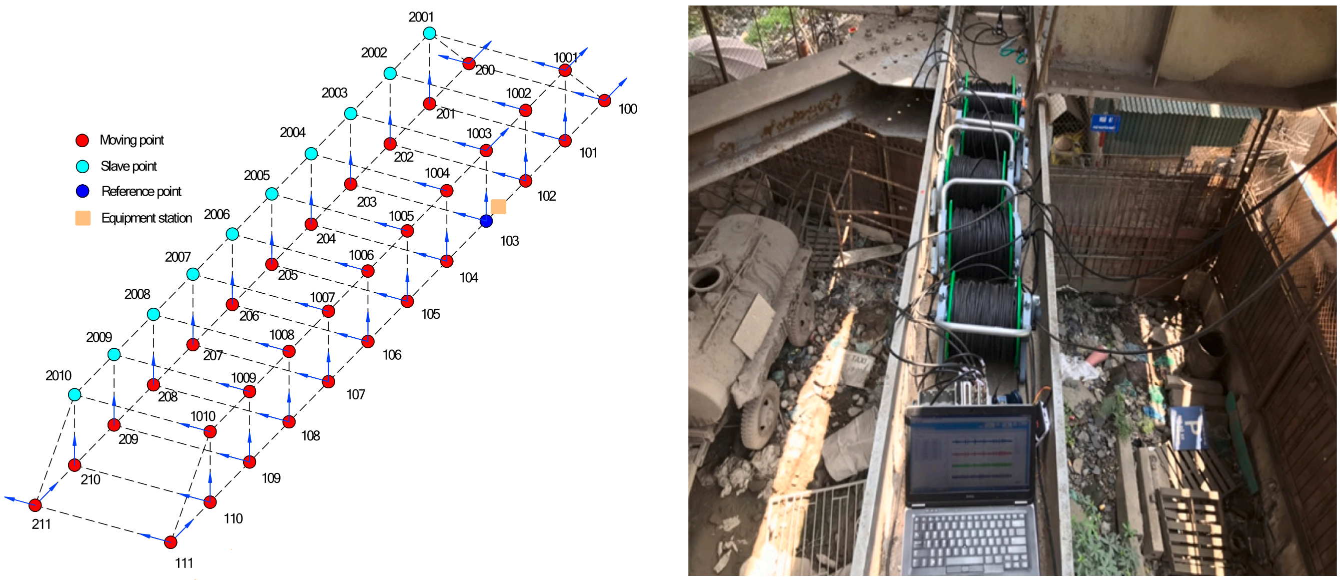

Fig. 14. Data collection at Chuong Duong bridge: a. Measurement point grid; b. Install measuring points on the site.

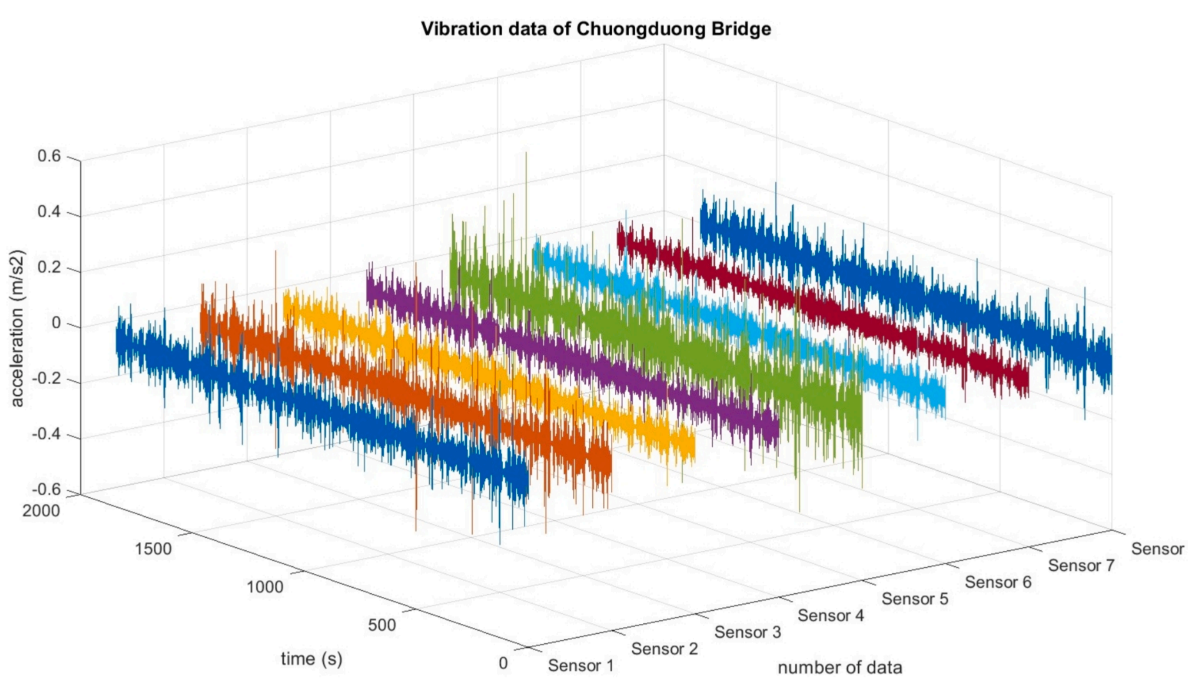

Fig. 15. Vibration data of one setup at Chuong Duong bridge.

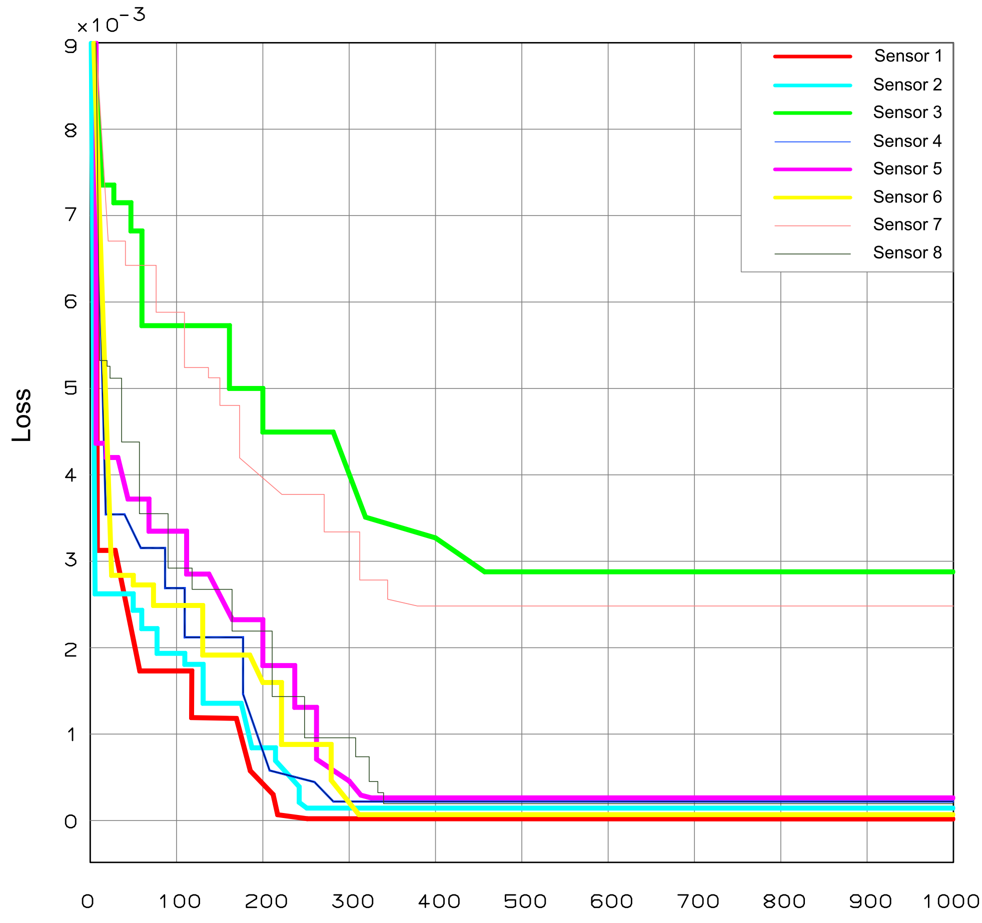

a.

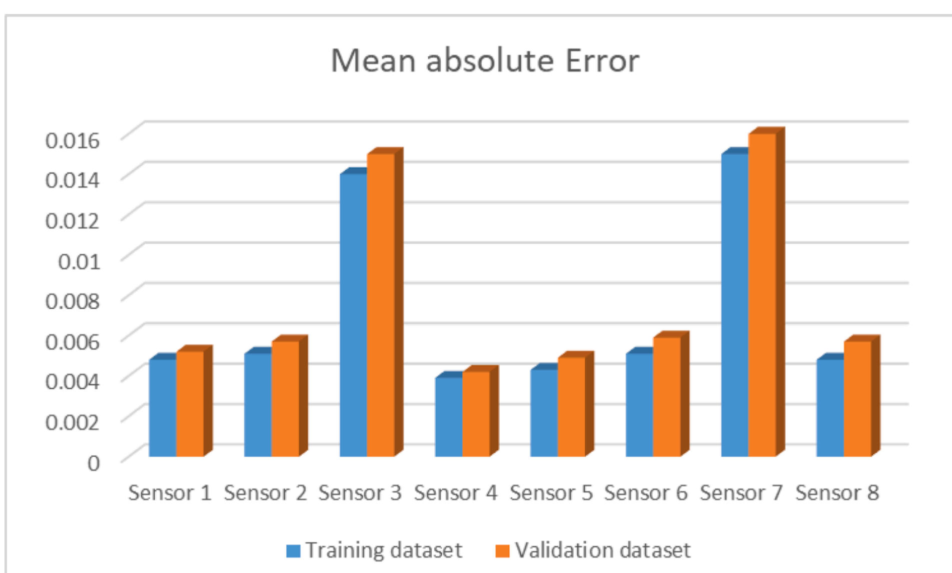

b.

Fig. 16. Data reconstruction at different locations: a. Loss training; b. Mean Absolute Error (MAE) of the best model.

the river with 11 steel truss spans, designed to accommodate heavy traffic flow. Built to alleviate traffic congestion, Chuong Duong Bridge has significantly contributed to maintaining smooth traffic flow into the city center. Since its completion, the bridge has not only eased the pressure on surrounding routes but also ensured efficient and uninterrupted transportation. To this day, the Chuong Duong Bridge remains a crucial part of Hanoi's transportation network, ensuring seamless connectivity and supporting the region's socio-economic development.

Chuong Duong Bridge was designed according to Vietnam's TCN18-79 standard [56]. It has an H30 load capacity for vehicles in the main lanes and an H6 load capacity for vehicles moving on the cantilevered sides of the bridge. The total cross-sectional width of the bridge is 20.6

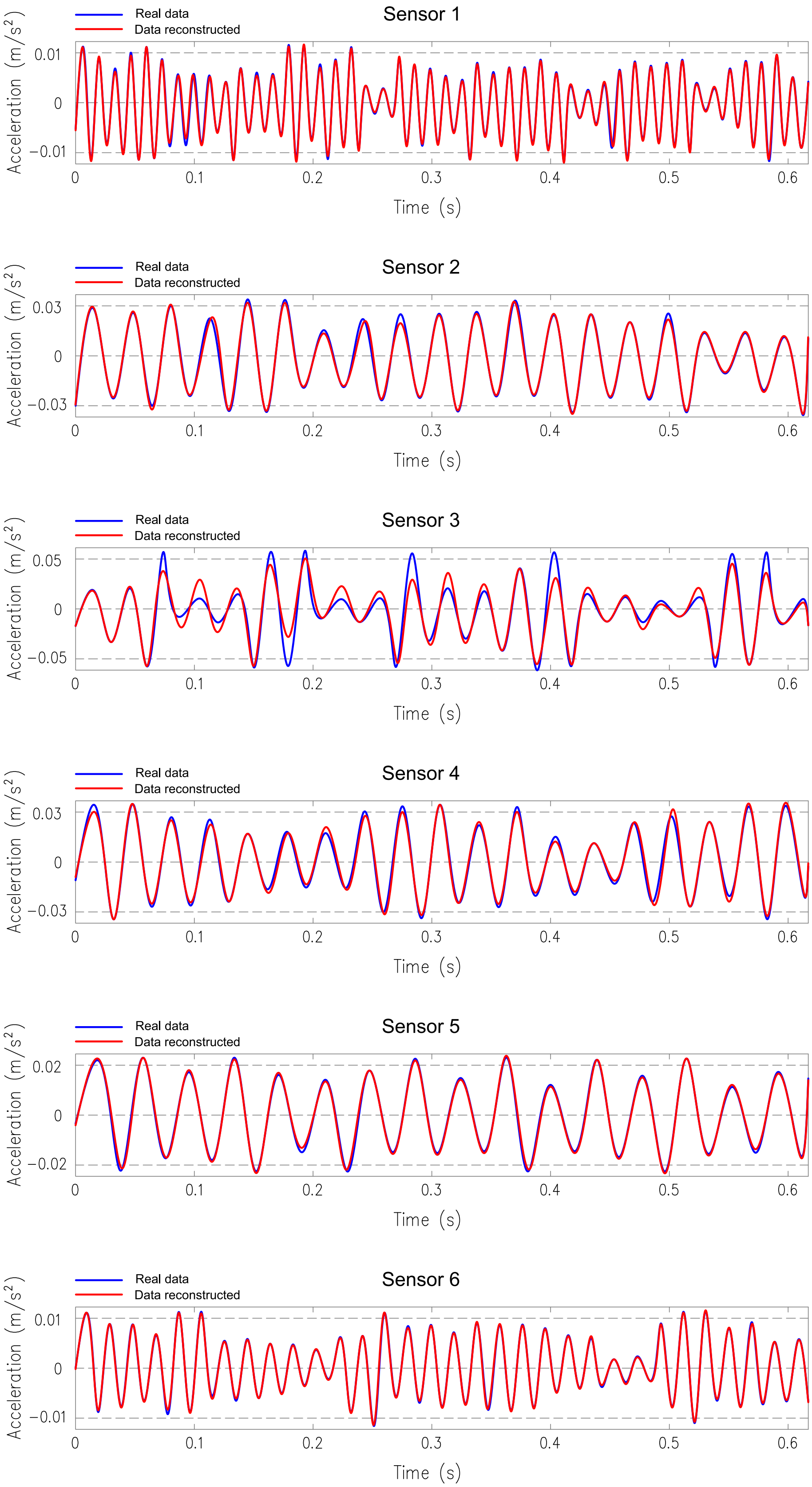

Fig. 17. Data reconstruction at different locations.

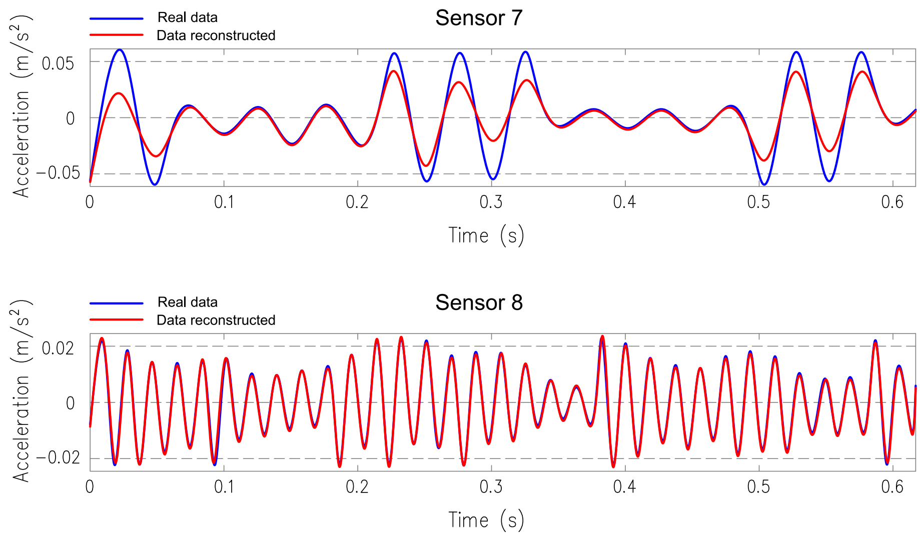

Fig. 17. (*continued*).

m. The truss members are H-shaped and are connected by plates at the truss joints. The deck system is supported by a network of transverse and longitudinal beams connected to the truss structure. The upper and lower bracing systems are designed to stabilize the bridge against both longitudinal and transverse loads.

Data gathering.

During the testing and load assessment campaign of the Chuong Duong Bridge, a comprehensive vibration data collection was conducted [23,57]. The equipment used was similar to that in the laboratory plate test, including 8 PCB accelerometers, an NI signal receiver, and other auxiliary devices. A comprehensive vibration measurement grid of the bridge was designed and divided into 8 sub-measurement rounds to optimize data collection (Fig. 14a). Measurement points were installed at the nodes of the bridge's truss, allowing data collection from the most critical structural locations (Fig. 14b). In space, the sensors were installed in three perpendicular directions: vertical, longitudinal, and transverse to the bridge.

A monitoring station was set up throughout the data collection process to supervise and control the entire operation. Random excitations, such as vehicles passing over the bridge, wind loads, and other factors, were utilized to induce natural vibrations in the bridge structure. Random vibration data collection setups were implemented. On-site, after each measurement setup was completed, the sensor data correlation was checked to ensure data quality. Simultaneously, the data was pre-processed to evaluate the results and ensure data quality. In case of any abnormalities, the setup was remade. Fig. 15 shows the data collected in one setup.

Data reconstruction

3.2.1. *Single channel data reconstruction*

In the case study involving an actual bridge structure, instead of comparing the performance of different machine learning models, this section will analyze and evaluate the data from different sensor locations. Scenarios involving data loss at various sensor positions will be conducted. Similar to the laboratory tests on plate structures, the collected data underwent preprocessing before being input into the model for training. The parameters of the proposed model are chosen similarly to the plate case: three 1DCNN layers, four LSTM layers, additional Max Pooling, and dropout layers. The results of the training process are shown in Fig. 16.

The convergence curve of the training process shown in Fig. 16a provides a preliminary assessment indicating that the 1DCNN-LSTM model performs well in most of the examined cases. After approximately 250–350 epochs, the model starts to gradually converge towards zero. Compared to the plate case discussed earlier, the model takes longer to converge. The data collection process from an actual bridge typically occurs under various conditions such as weather, temperature, and bridge activity, leading to greater variability in the data. These factors necessitate the model to process and filter out more noise signals, thereby extending the convergence time of the training process. Working with more complex real-world data also poses a greater challenge for the model in accurately identifying and reconstructing useful signals from the raw data. This can explain the longer convergence time compared to the plate structure in the laboratory setting.

At the bridge bearings (located above the expansion joints), signals are frequently disturbed by external forces, particularly the impact of vehicles crossing the expansion joints. This adds complexity to the data at these locations. Sensors 3 and 7, installed at the bridge bearings, exhibit lower performance compared to other sensors. The convergence curves for reconstructing data from these two sensors take the longest to converge, highlighting the complexity of the data at these noisy positions. Despite this, the 1DCNN-LSTM model still operates and can reconstruct data at these locations, although its performance is significantly reduced compared to less noisy positions. This indicates that while the proposed model can handle data from complex real-world environments, further optimization is needed to improve its performance in high-noise areas.

Fig. 16b shows the average difference between the actual and reconstructed values in different scenarios. Fig. 15b also demonstrates the accuracy of the reconstructed data across various cases. The reconstructed values are relatively accurate in both the training and test sets. However, the cases of sensor 3 and sensor 7, located at the bridge bearings, have lower accuracy compared to the other cases. This corresponds with the longer convergence time observed for these sensors, indicating challenges due to the noisy environment. Despite this, the model still achieves commendable performance in reconstructing data from most sensors, suggesting that while the proposed 1DCNN-LSTM model is effective, improvements are needed to handle data from particularly noisy locations. Fig. 17 shows a portion of the reconstructed data at different locations.

At regular positions, the reconstructed data closely matches the actual data, showing the model's effectiveness in most scenarios. However, at the bearing positions, specifically at sensors 3 and 7, where data exhibits sudden changes, the reconstructed data does not align well with the actual data.

A modal analysis was conducted to assess the reliability of the reconstructed data. This analysis aimed to examine the accuracy and reliability of the data after it was reconstructed by 1DCNN-LSTM,

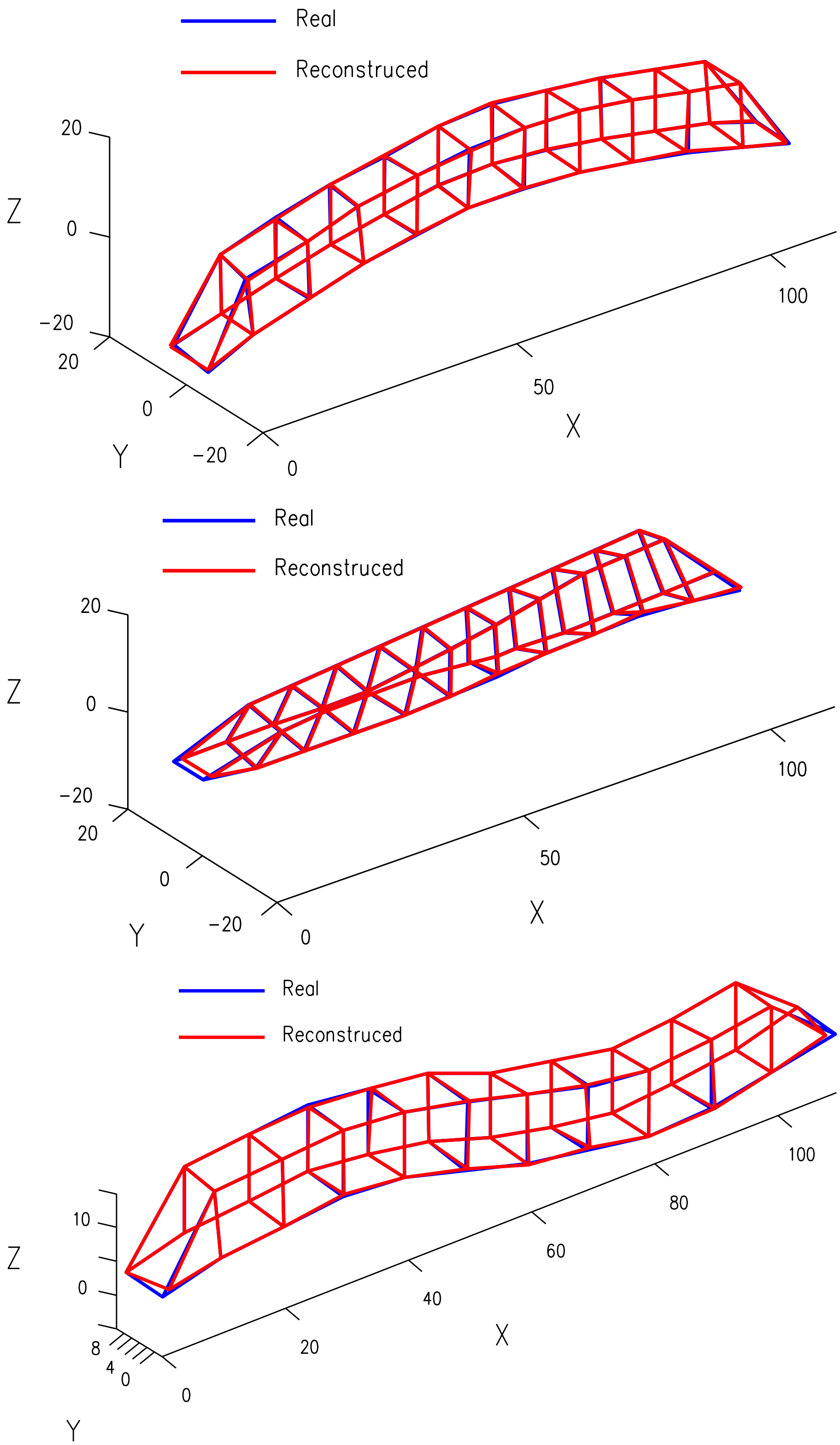

Fig. 18. Mode shape results of Chuong Duong bridge with 2 datasets: a. Mode 1; b. Mode 2; c. Mode 3; d. Mode 4; e. Mode 5; f. Mode 6 (Compare with actual values in [23]).

determining whether the reconstructed values accurately reflect the characteristics and behavior of the actual data. The results of the analysis are presented in Fig. 18 and Table 4.

The mode shapes obtained from the analysis of both the actual and reconstructed datasets show a high degree of similarity. The locations of the vibration points almost coincide, with the overall mode shape appearing nearly identical between the two datasets. Notably, the greatest differences are observed at the bridge bearings. These results

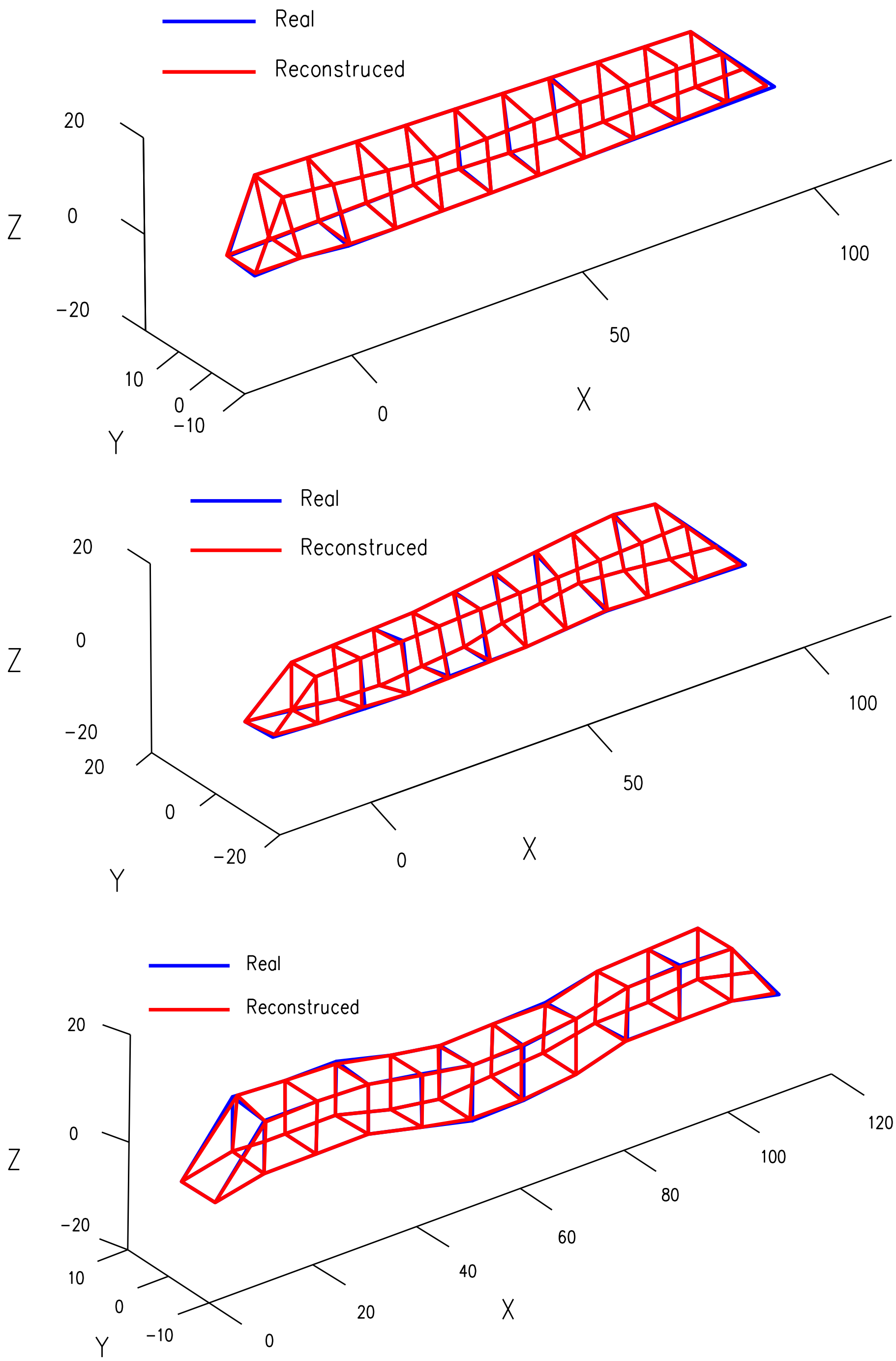

Fig. 18. (*continued*).

Table 4
Results of analysis of real and reconstruction data at Chuong Duong bridge.

Mode	Frequency		Error (%)	MAC
	Real data	Reconstructed data		
1st	1.79	1.77	1.117	0.989
2nd	3.57	3.62	1.401	0.987
3rd	4.30	4.42	2.791	0.988
4th	4.60	4.51	1.957	0.986
5th	5.03	5.19	3.181	0.983
6th	8.09	7.99	1.236	0.985

indicate that the model effectively captures the essential characteristics of the structure's response, although it struggles more in areas subjected to higher noise levels, such as the bridge bearings. The consistency in mode shapes across other regions demonstrates the robustness of the proposed 1DCNN-LSTM model in accurately reconstructing sensor data for structural health monitoring.

Observing Table 4, the frequency of the bridge structure obtained from the analysis and comparison of the two datasets shows minor differences. Specifically, in the fourth mode shape, the frequency exhibits the largest difference, but it is only 3.181 %. Although the data from the actual structure, after analysis, show greater discrepancies compared to the lab-based plate, the differences are not significant. This indicates that the model is capable of reconstructing data with high accuracy,

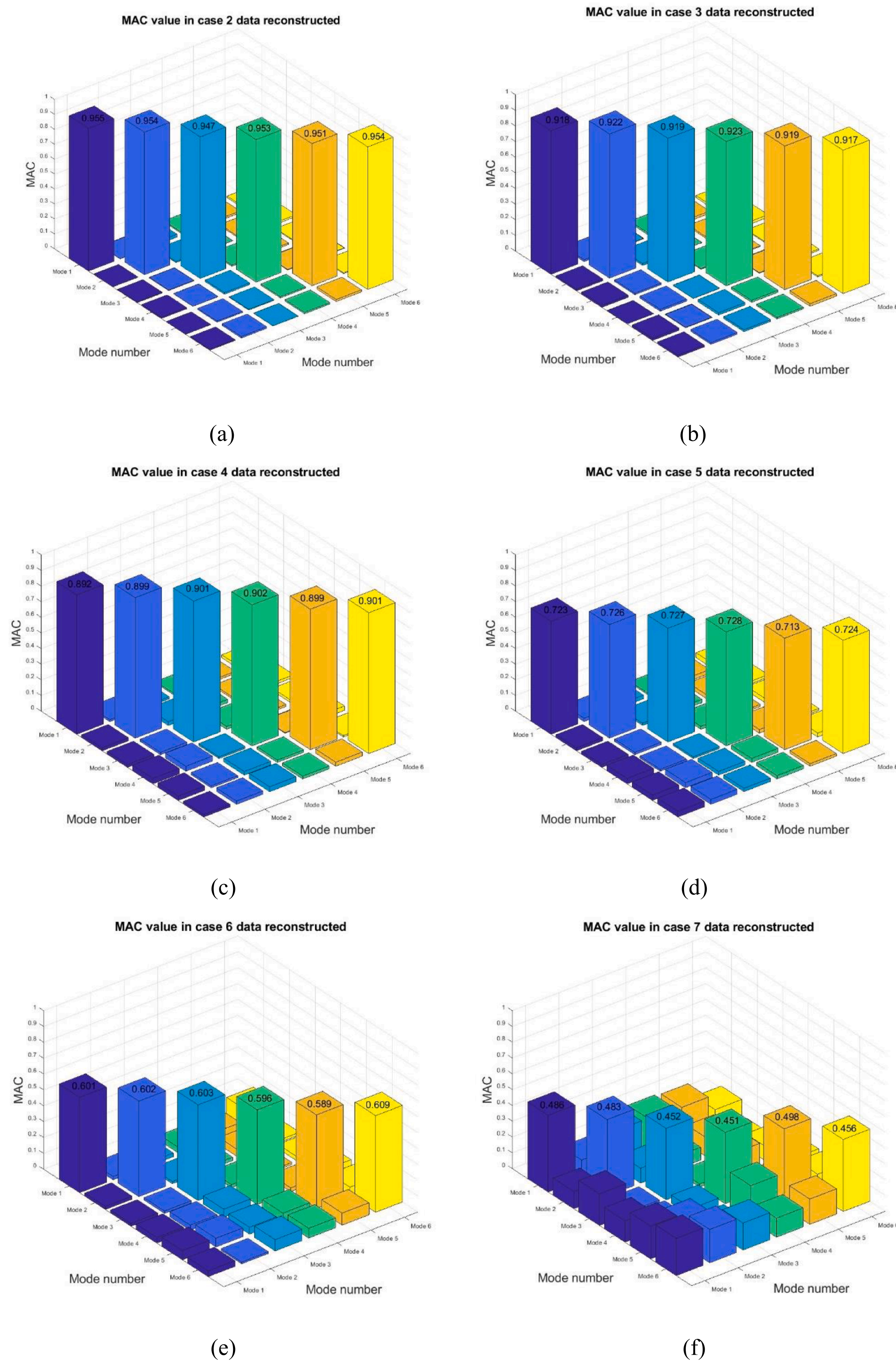

Fig. 19. MAC value in data loss scenarios of the Chuong Duong dataset.

even though the data collected from the actual structure is more complex than laboratory conditions.

Furthermore, the MAC values also achieve high scores, close to 1. This indicates that the reconstructed dataset is highly representative of the real data. The small discrepancy in frequency, combined with high MAC values, demonstrates that the proposed 1DCNN-LSTM model maintains its effectiveness in analyzing the dynamic characteristics of the bridge structure, confirming the feasibility of the method for practical applications. The high MAC values reinforce the reliability of the reconstructed data in accurately reflecting the behavior and characteristics of the actual structure, thereby validating the robustness and precision of the model in real practical scenarios.

3.2.2. Multi-channel data reconstruction

The multichannel data reconstruction for the Chuong Duong Bridge was carried out using a similar method to that employed for the plate in the previous case study. Accordingly, the data from the sensors were sequentially corrupted (assigned a value of 0), and then data reconstruction was performed.

Fig. 19 illustrates the MAC values for various data loss scenarios after mode analysis. Overall, the network's performance decreased compared to the laboratory data set but still achieved relatively high efficiency. Specifically, for the Chuong Duong Bridge data set, the highest MAC value achieved in the case of reconstructing data from 2 sensors was 0.955 (while for the laboratory plate, it was 0.969). Other cases also showed a decrease in MAC values compared to the laboratory study. This can be attributed to the complexity and variability of real-world data from the bridge, which includes more noise and fluctuations than the controlled laboratory environment. However, the MAC values obtained remain high, demonstrating the model's ability to accurately reconstruct sensor data in complex real conditions. Despite some decrease, these results indicate that the data reconstruction method can still be effectively applied in practical situations.

As the number of faulty sensors increases, the model's performance and accuracy decrease significantly in each case. Specifically, when there are 3 faulty sensors, the MAC value drops to 0.923, and when the number of faulty sensors increases to 4, this value further decreases to 0.901. This trend continues to worsen with more faulty sensors, with the MAC value reaching only 0.728 when 5 sensors are faulty and dropping sharply to 0.609 with 6 non-functional sensors. Particularly, in the most severe scenario with 7 faulty sensors, the MAC value is only 0.498. This decrease indicates that although the 1DCNN-LSTM model can relatively accurately reconstruct data from sensors, it struggles significantly when faced with severe data loss. This highlights the need for improving and optimizing the model to ensure higher performance in more complex data loss scenarios.

4. Conclusion

This research introduces a novel approach that combines 1DCNN and LSTM for sensor data reconstruction in SHM. The proposed method uses the strengths of 1DCNN in feature extraction and LSTM's ability to process time-series data. The effectiveness of this combination is demonstrated through two case studies, confirming the significant efficiency of the 1DCNN-LSTM model. From these studies, several key conclusions are drawn:

(1) The 1DCNN-LSTM combined method provides high performance in sensor data reconstruction for SHM compared to other machine learning models with the same input parameters. This improvement is clearly demonstrated through the accuracy and reliability of the reconstructed data, making the 1DCNN-LSTM approach more effective in handling complex structural health monitoring scenarios.
(2) For single-channel data reconstruction, the proposed method achieves relatively high accuracy when applied to both laboratory and real practical datasets. Although the effectiveness of the method decreases slightly when applied to real bridge structural data, it still maintains a high level of accuracy.
(3) The proposed method demonstrates the ability to effectively reconstruct data from one or multiple faulty sensors. However, as the number of faulty sensors increases, the model's performance tends to decrease.
(4) Future research could focus on enhancing the network's performance and expanding the method's applicability to different types of sensor data. To achieve this, studies could investigate advanced network optimization techniques, such as improving network architecture or fine-tuning training parameters, to achieve better performance under real-world conditions.

CRediT authorship contribution statement

T.Q Minh: Writing – review & editing, Writing – original draft, Visualization, Validation, Software, Methodology, Investigation, Data curation, Conceptualization. **Jose C. Matos:** Writing – review & editing, Supervision, Methodology, Conceptualization. **Helder S. Sousa:** Writing – review & editing, Supervision, Data curation, Conceptualization. **Son Dang Ngoc:** Writing – review & editing, Validation, Methodology, Data curation, Conceptualization. **Thuc Ngo Van:** Writing – review & editing, Writing – original draft, Validation, Data curation. **Huan X. Nguyen:** Writing – review & editing, Visualization, Supervision, Data curation. **Quyền Nguyễn:** Writing – review & editing, Supervision, Resources, Methodology, Funding acquisition, Formal analysis, Conceptualization.

Declaration of competing interest

The authors declare that they have no known competing financial interests or personal relationships that could have appeared to influence the work reported in this paper.

Acknowledgments

The authors are grateful to the UCT company for their support. The first author acknowledges the support of the doctoral grant reference PRT/BD/154268/2022, financed by the Portuguese Foundation for Science and Technology (FCT) under the MIT Portugal Program (2022 MPP2030-FCT). The corresponding author acknowledges the financial support from the National Foundation for Science and Technology of Portugal (FCT) with the reference CEECINST/00156/2018/CP1642/CT0013 (DOI: 10.54499/CEECINST/00156/2018/CP1642/CT0013) at the Centre for Textile Science and Technology (2C2T) of the School of Engineering at the University of Minho. The fifth author acknowledges the Post-Doctoral Scholarship Programme of Vingroup Innovation Foundation (VINIF, Vietnam), code VINIF.2024.STS.06. This work was partly financed by the National Foundation for Science and Technology of Portugal (FCT) and Technology and Higher Education (MCTES), through national funds (PIDDAC) under the R&D Unit Institute for Sustainability and Innovation in Structural Engineering (ISISE), under reference UIDB/04029/2020 (doi.org/10.54499/UIDB/04029/2020), and under the Associate Laboratory Advanced Production and Intelligent Systems ARISE under reference LA/P/0112/2020.

Data availability

The authors do not have permission to share data.

References

[1] TN. Bittencourt, D. Frangopol, A. Beck, "Maintenance, monitoring, safety, risk and resilience of bridges and bridge networks,", CRC Press (2016) https://doi.org/10.1201/9781315207681.

[2] S.S. Saidin, A. Jamadin, S. Abdul Kudus, et al., An overview: the application of vibration-based techniques in bridge structural health monitoring, Int J Concr Struct Mater (2022), https://doi.org/10.1186/s40069-022-00557-1.
[3] B.T. Svendsen, O. Øiseth, G.T. Frøseth, A. Rønnquist, A hybrid structural health monitoring approach for damage detection in steel bridges under simulated environmental conditions using numerical and experimental data, Struct. Health Monit. (2023), https://doi.org/10.1177/14759217221098998.
[4] Andrei et al, "Static and Dynamic Structural Health Monitoring System for Bridges," *Romanian Journal of Transport Infrastructure*, 2021, Doi: 10.2478/rjti-2021-0007.
[5] Comisu et al., "Structural health monitoring system of bridges," *Procedia Engineering*, Doi: 10.1016/j.proeng.2017.09.472.
[6] Kai-Yuen Wong, "Design of a structural health monitoring system for long-span bridges," *Structure and Infrastructure Engineering: Maintenance, Management, Life-Cycle Design and Performance*, doi: https://doi.org/10.1080/15732470600591117.
[7] "Integrated structural health monitoring in bridge engineering," *Automation in Construction*, 2022, Doi: 10.1016/J.AUTCON.2022.104168.
[8] Tran et al, "Finite Element Model Updating for Composite Plate Structures Using Particle Swarm Optimization Algorithm," *Appl. Sci*, 2023, Doi: 10.3390/app13137719.
[9] Nguyen et al, "Damage detection of structural based on indirect vibration measurement results combined with Artificial Neural Network," *Journal of Materials and Engineering Structures « JMES »*, 2022, doi: http://revue.ummto.dz/index.php/JMES/article/view/3286.
[10] S. Vasavi, G. Lasya Sravanthi, B. Sai Ram, A. Anu Gokhale, "Predictive analytics of bridge safety for intelligent transportation system using ensemble model," *Materials Today: Proceedings*, 2021, Doi: 10.1016/j.matpr.2021.02.348.
[11] Y. Kaya, E. Safak, Real-time analysis and interpretation of continuous data from structural health monitoring (SHM) systems, Bull Earthquake Eng (2015), https://doi.org/10.1007/s10518-014-9642-9.
[12] C.S. Shim, N.S. Dang, S. Lon, C.H. Jeon, Development of a bridge maintenance system for prestressed concrete bridges using 3D digital twin model, Struct. Infrastruct. Eng. (2019), https://doi.org/10.1080/15732479.2019.1620789.
[13] G. SWang, J. Ke, Literature Review on the Structural Health Monitoring (SHM) of Sustainable Civil Infrastructure: an Analysis of Influencing Factors in the Implementation, Buildings (2024), https://doi.org/10.3390/buildings14020402.
[14] Y. Deng, Y. Zhao, H. Ju, T.H. Yi, A. Li, Abnormal data detection for structural health monitoring: State-of-the-art review, Dev. Built Environ. (2024), https://doi.org/10.1016/J.DIBE.2024.100337.
[15] K. Jiang, Q. Han, Du. Xiuli, P. Ni, Structural dynamic response reconstruction and virtual sensing using a sequence to sequence modeling with attention mechanism, Autom. Constr. (2021), https://doi.org/10.1016/j.autcon.2021.103895.
[16] N. Makhoul, Review of data quality indicators and metrics, and suggestions for indicators and metrics for structural health monitoring, Adv. Bridge Eng. (2022), https://doi.org/10.1186/s43251-022-00068-9.
[17] S.-Y. Chen, Y.-W. Wang, Y.-Q. Ni, Gross outlier removal and fault data recovery for SHM data of dynamic responses by an annihilating filter-based Hankel-structured robust PCA method, Struct. Control Health Monit. (2022), https://doi.org/10.1002/stc.3144.
[18] P.J. García-Laencina, J.L. Sancho-Gómez, A.R. Figueiras-Vidal, Pattern classification with missing data: a review, Neural Comput & Applic (2010), https://doi.org/10.1007/s00521-009-0295-6.
[19] P. Royston, I.R. White, Multiple Imputation by Chained Equations (MICE): Implementation in Stata, J. Stat. Softw. (2011), https://doi.org/10.18637/jss.v045.i04.
[20] M.F. Shaikh, K. Nallasivam, Dynamic response of a box-girder bridge using the finite element technique, Asian J Civ Eng (2023), https://doi.org/10.1007/s42107-023-00633-1.
[21] V. Zanjani Zadeh, A. Patnaik, Finite element modeling of the dynamic response of a composite reinforced concrete bridge for structural health monitoring, Int J Adv Struct Eng (2014), https://doi.org/10.1007/s40091-014-0055-4.
[22] N.F. Alkayem, M. Cao, Y. Zhang, et al., Structural damage detection using finite element model updating with evolutionary algorithms: a survey, Neural Comput & Applic (2018), https://doi.org/10.1007/s00521-017-3284-1.
[23] M.Q. Tran, H.S. Sousa, T.V. Ngo, B.D. Nguyen, Q.T. Nguyen, H.X. Nguyen, E. Baron, J. Matos, S.N. Dang, Structural assessment based on vibration measurement test combined with an artificial neural network for the steel truss bridge, Appl. Sci. (2023), https://doi.org/10.3390/app13137484.
[24] L.V. Ho, S. Khatir, G.D. Roeck, T. Bui-Tien, M.A. Wahab, Finite element model updating of a cable-stayed bridge using metaheuristic algorithms combined with Morris method for sensitivity analysis, Smart Struct. Syst. (2020), https://doi.org/10.12989/SSS.2020.26.4.451.
[25] Minh et al, "Effect of bridge foundation stiffness on dynamic behavior of bridge structure," *IABSE Congress New Delhi 2023*, 2023, doi: 10.2749/newdelhi.2023.0500.
[26] J. Brownlee, Deep learning for time series forecasting predict the future with MLPs, Cnns and LSTMs in Python. (2018). https://machinelearningmastery.com/deep-learning-for-time-series-forecasting/.
[27] PB. Weerakody, KW. Wong, G. Wang, W. Ela, "A review of irregular time series data handling with gated recurrent neural networks,", Neurocomputing (2021) https://doi.org/10.1016/j.neucom.2021.02.046.
[28] A. Casolaro, V. Capone, G. Iannuzzo, F. Camastra, Deep learning for time series forecasting: advances and open problems, Information (2023), https://doi.org/10.3390/info14110598.
[29] Moreno, Emilio Ruiz, "Machine Learning for Signal Reconstruction from Streaming Time-series Data," University of Agder, 2024. [Online]. Available: https://hdl.handle.net/11250/3114510.
[30] C. Chen, et al., Reconstruction of long-term strain data for structural health monitoring with a hybrid deep-learning and autoregressive model considering thermal effects, Eng. Struct. (2023), https://doi.org/10.1016/j.engstruct.2023.116063.
[31] B. Oh, H. Park, B. Glisic, Prediction of long-term strain in concrete structure using convolutional neural networks, air temperature and time stamp of measurements, Automat Constr (2021), https://doi.org/10.1016/j.autcon.2021.103665.
[32] X. Lei, L. Sun, Y. Xia, Lost data reconstruction for structural health monitoring using deep convolutional generative adversarial networks, Struct Health Monit (2021), https://doi.org/10.1177/1475921720959226.
[33] Q. Tang, Y. Jiang, J. Xin, G. Liao, J. Zhou, X. Yang, A novel method for the recovery of continuous missing data using multivariate variational mode decomposition and fully convolutional networks, Measurement (2023), https://doi.org/10.1016/j.measurement.2023.113366.
[34] Jingzhou Xin, Chaoying Zhou,Yan Jiang, Qizhi Tang,Xianyi Yang, Jianting Zhou, "A signal recovery method for bridge monitoring system using TVFEMD and encoder-decoder aided LSTM," *Measurement*, 2023, Doi: 10.1016/j.measurement.2023.112797 Get rights and content.
[35] Jiang et al, "Continuous missing data imputation with incomplete dataset by generative adversarial networks–based unsupervised learning for long-term bridge health monitoring," *Structural Health Monitoring*, 2021, Doi: 10.1177/14759217211021942.
[36] Yangtao Li , Tengfei Bao, Zexun Chen, Zhixin Gao, Xiaosong Shu, Kang Zhang, "A missing sensor measurement data reconstruction framework powered by multi-task Gaussian process regression for dam structural health monitoring systems," 2021, Doi: 10.1016/j.measurement.2021.110085.
[37] Y. Wang, Du. Taili, Y. Guo, F. Dong, J. Si, Xu. Minyi, A novel Kalman smoothing (Ks) − Long Short-Term Memory (LSTM) hybrid model for filling in short- and long-term missing values in significant wave height, Measurement (2025), https://doi.org/10.1016/j.measurement.2024.115947.
[38] Y.-K. Zhu, H.-P. Wan, M.D. Todd, A method for reconstruction of structural health monitoring data using WGANGP with U-net generator, Struct. Health Monit. (2025), https://doi.org/10.1177/14759217241313438.
[39] H.-P. Wan, Y.-Q. Ni, Bayesian multi-task learning methodology for reconstruction of structural health monitoring data, Struct. Health Monit. (2018), https://doi.org/10.1177/1475921718794953.
[40] Y. Lu, L. Tang, C. Chen, L. Zhou, Z. Liu, Y. Liu, et al., Reconstruction of long-term acceleration response for long-span bridges based on BiLSTM networks, Eng Struct (2023), https://doi.org/10.1016/j.engstruct.2023.116000.
[41] G. Fan, J. Li, H. Hao, Lost data recovery for structural health monitoring based on convolutional neural networks, Struct Control Health Monit (2019), https://doi.org/10.1002/stc.2433.
[42] B. Oh, B. Glisic, Y. Kim, H. Park, Convolutional neural network-based data recovery method for structural health monitoring, Struct Health Monit (2020), https://doi.org/10.1177/1475921719897571.
[43] N.T.C. Nhung, H.B. Nguyen, T.Q. Minh, Reconstructing health monitoring data of railway truss bridges using one-dimensional convolutional neural networks, Eng. Technol. Appl. Sci. Res., (2024), https://doi.org/10.48084/etasr.7515.
[44] Osama Abdeljaber ,Onur Avci, Serkan Kiranyaz, Moncef Gabbouj, Daniel J. Inman, "Real-time vibration-based structural damage detection using one-dimensional convolutional neural networks," *Journal of Sound and Vibration*, Doi: 10.1016/j.jsv.2016.10.043.
[45] J. Zhang, M. Huang, N. Wan, Z. Deng, Z. He, J. Luo, Missing measurement data recovery methods in structural health monitoring: The state, challenges and case study, Measurement (2024), https://doi.org/10.1016/j.measurement.2024.114528.
[46] E.U.H. Qazi, A. Almorjan, T.A. Zia, "A One-Dimensional Convolutional Neural Network (1D-CNN) based deep learning system for network intrusion detection,", Appl. Sci. (2022) https://doi.org/10.3390/app12167986.
[47] T. Çavdar, N. Ebrahimpour, M.T. Kakız, et al., Decision-making for the anomalies in IIoTs based on 1D convolutional neural networks and Dempster–Shafer theory (DS-1DCNN), Supercomput (2023), https://doi.org/10.1007/s11227-022-04739-2.
[48] Wang et al, "A hybrid deep learning model with 1DCNN-LSTM-Attention networks for short-term traffic flow prediction," *Physica A: Statistical Mechanics and its Applications*, 2021, Doi: 10.1016/j.physa.2021.126293.
[49] Jason Brownlee, "Deep Learning for Time Series", doi: https://machinelearningmastery.com/category/deep-learning-time-series/.
[50] H. Sepp, S. Jürgen, Long short-term memory, Neural Comput. (1997), https://doi.org/10.1162/neco.1997.9.8.1735.
[51] K. Zarzycki, M. Ławryńczuk, LSTM and GRU neural networks as models of dynamical processes used in predictive control: a comparison of models developed for two chemical reactors, Sensors (2021), https://doi.org/10.3390/s21165625.
[52] Jason Brownlee, "How to Develop a Bidirectional LSTM For Sequence Classification in Python with Keras", doi: https://machinelearningmastery.com/develop-bidirectional-lstm-sequence-classification-python-keras/.
[53] UCT company, "Consulting report on inspection, assessment of causes and preparation of a feasibility study report in the preparation of the Thang Long bridge repair project - Báo cáo tư vấn kiểm định, đánh giá nguyên nhân và lập báo cáo nghiên cứu khả thi thuộc công tác chuẩn bị dự án sửa chữa cầu Thăng Long," 2021.
[54] Long Viet Ho, Trang Thi Trinh, Guido De Roeck, Thanh Bui-Tien, Long Nguyen-Ngoc, Magd Abdel Wahab, "An efficient stochastic-based coupled model for

damage identification in plate structures," 2022, Doi: 10.1016/j.engfailanal.2021.105866.

[55] Edwin Reynders, Mattias Schevenels, Guido De Roeck, "Macec - The matlab toolbox for experimental and operational modal analysis," vol. MACEC 3.4, [Online]. Available: https://bwk.kuleuven.be/bwm/macec/macec.pdf.

[56] TCVN/QCVN, *Industry Standard 22TCN 18-79 Bridge and Culvert Design Procedures According to Limit State Issued under Decision No. 2057 QD/KT4 dated September 19, 1979 - Tiêu Chuẩn Ngành 22TCN 18-79 Quy Trình Thiết Kế Cầu Cống Theo Trạng Thái Giới Hạn Ban hành theo Quyết định số 2057 QĐ/KT4 ngày 19/9/1979*, 1979.

[57] UCT company, "Chuong Duong bridge load test report - Báo cáo kiểm định thử tải cầu Chương Dương," 2022.